2

6

NASA TECHNICAL NOTE

NASA TN D-7174

STUDIES RELATING TO TEMPERATURE CONTROL OF A LARGE SPACE TELESCOPE

by S. Katzoff

Langley Research Center
Hampton, Va. 23365

63

1. Report No. NASA TN D-7174	2. Government Accession No.	3. Recipient's Catalog No.
4. Title and Subtitle STUDIES RELATING TO TEMPERATURE CONTROL OF A LARGE SPACE TELESCOPE		5. Report Date February 1973
		6. Performing Organization Code
7. Author(s) S. Katzoff		8. Performing Organization Report No. L-8741
9. Performing Organization Name and Address NASA Langley Research Center Hampton, Va. 23365		10. Work Unit No. 188-78-57-05
		11. Contract or Grant No.
12. Sponsoring Agency Name and Address National Aeronautics and Space Administration Washington, D.C. 20546		13. Type of Report and Period Covered Technical Note
		14. Sponsoring Agency Code

15. Supplementary Notes

16. Abstract

Analytical methods are developed for estimating the circumferential and longitudinal temperature distributions in a large space telescope, idealized as a simple insulated tube with a flat mirror across one end. The effects of wall conduction, multilayer insulation, thermal coatings, heat pipes, and heated collars are analyzed, with numerical examples. For most of the study, the only thermal input to the tube was assumed to be from steady solar irradiation from one side, as in a geosynchronous orbit. Unsteady heat flow through the insulation, as in alternating sunlight and shadow of a low orbit, is briefly discussed.

17. Key Words (Suggested by Author(s)) Astronomical telescopes Configuration factors — cylinders Heat pipes Integral equations Multilayer insulation Radiation exchange Radiative heat transfer Temperature control View factors — cylinders	18. Distribution Statement Unclassified — Unlimited		
19. Security Classif. (of this report) Unclassified	20. Security Classif. (of this page) Unclassified	21. No. of Pages 61	22. Price* $3.00

CONTENTS

Preceding page blank

STUDIES RELATING TO TEMPERATURE CONTROL
OF A LARGE SPACE TELESCOPE

By S. Katzoff
Langley Research Center

SUMMARY

Analytical methods are developed for estimating the circumferential and longitudinal temperature distributions in a large space telescope, idealized as a simple insulated cylindrical tube with a flat mirror across one end. The basic variable is σT^4, where σ is the Stefan-Boltzmann constant and T is the absolute temperature. The circumferential distribution is found as a Fourier series. With the view factor between circular bands of the tube approximated by a simple exponential, the longitudinal distribution is then found as an exponential expression.

The effects of wall conduction, multilayer insulation, thermal-coating characteristics, heat pipes, and heated collars are analyzed, with numerical examples. The effects of nonuniform coatings and insulation are also discussed. A brief analysis is also given of unsteady heat flow through the insulation, as in alternate light and shadow of a low orbit. The numerical examples were mostly simplified by assuming that the only external thermal input was from solar radiation directed at right angles to the tube axis.

Multilayer insulation around the large tube can limit the circumferential temperature nonuniformity to tenths of a degree. Adding circumferential heat pipes can reduce it further, to hundredths of a degree. The insulation, however, lowers the tube temperature and causes a pronounced drop in temperature along the tube toward the open end. A heated collar around the inside of the tube near the open end can overcome this problem and provide a nearly uniform temperature along the tube between the mirror and the collar.

INTRODUCTION

Among the more ambitious of the space-science proposals that are under study by various research groups is the diffraction-limited Large Orbiting Telescope (LOT), or Large Space Telescope (LST), more or less as it was proposed by Lyman Spitzer, Jr., some years ago. (See ref. 1.) The extent and intensity of interest in such a telescope are attested by the many papers dealing with the various facets of its design and construction that were presented in a 1969 workshop on optical telescope technology. (See ref. 2.)

1

As was pointed out in reference 1, maintaining diffraction-limited optics in a telescope of, say, a 3-meter or larger diameter, implies an extremely fine temperature control in order to avoid thermal distortions. Temperature uniformity and constancy to within a small fraction of a degree may be required. However, the availability of materials with very low thermal coefficients of expansion should help to alleviate the problem. Active optics (that is, continuously adjustable mirror figure and alinement) is an additional approach to alleviating the problem. (See ref. 3.) Heat pipes, vapor chambers, phase-change materials, thermal shields and enclosures, multilayer insulations, and automatic shutters may also find application in solving the thermal problem.

The present paper is an analytical study of the thermal problem for a simple idealized configuration that should serve as a first approximation to any eventual design. Specifically, the configuration is essentially a cylindrical tube with its inner surface perfectly black, and with a flat, perfectly reflecting mirror at its closed end. (See sketch (a).) The axis is assumed to be normal to the solar radiation for most of the analyses. Although the large telescope would probably be of the Cassegrain type, no effort has been made to take into account the presence of the secondary mirror or of the hole at the center of the primary mirror. This simplification should not greatly affect the usefulness of the analysis and results.

Sketch (a)
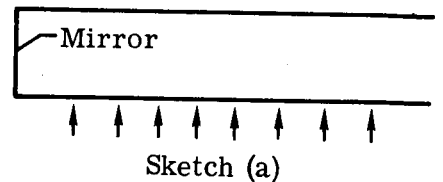
This study has two purposes: (1) to present analytical methods that are available for making such a study, and (2) to present enough numerical results to indicate the degree of temperature uniformity attainable by the various means discussed. The analytical methods concern the determination of circumferential and longitudinal temperature distributions in the tube wall. The analysis of the circumferential distribution involves a Fourier-series approach; the analysis of the longitudinal distribution involves use of an exponential view factor between circular bands in the cylinder. None of the methods described require more computer capability than is available in a programable desk-top calculator.

Steady-state conditions were assumed for nearly all cases. As previously indicated, for most of the calculations the cylinder axis was taken as normal to the solar rays, and the shaded half of the cylinder was assumed to receive no radiation at all. The effects of insulation, thermal coating, heat pipes, and heated collars were considered. A few calculations concerning the effect of alternating sunlight and shadow, as in a typical low orbit, were also made. No effort was made to cover wide ranges of the parameters and of their various combinations. However, the results should be adequate for showing the main aspects of the problem.

Some of the results given in this paper were presented previously in a paper at the workshop (ref. 4). The analytical methods, however, were not described in that paper.

This paper should be recognized as fairly limited in both purpose and scope. It mainly concerns the temperature of the telescope tube. If this temperature can be maintained uniform and constant, the uniformity and constancy will be reflected in (1) the radiation striking the face of the primary mirror, (2) the radiation environment of the secondary mirror, and (3) the alinement of the secondary mirror with the primary mirror. But even within this limited purpose of the paper, some important pertinent problems have not be analyzed — for example, the use of a removable cover for the tube opening.

SYMBOLS

A,B,C   constants in expressions for $z(x)$ and $y(x)$ (for finite-length tube)

a   circumferential mean value of z on outer layer of insulation (for finite-length tube)

a_n coefficient of $\cos n\theta$ in Fourier series for z

a_0 mean value of z around infinite cylinder

b   solar constant, $\dfrac{1}{30}$ cal/cm^2-sec

C   thermal conductivity of wall material, cal/cm-sec-K

$c = \dfrac{k\epsilon}{k + \epsilon}$

$\cos^* \theta$ function defined by equation (6)

$f = \sqrt{\dfrac{c}{1 + c}}$

$g = \dfrac{c\epsilon_i}{\epsilon_i + \rho_i c}$

$h = \sqrt{\dfrac{g}{1 + g}}$

k   "radiation conductance" of multilayer insulation (Rate of heat transmission is $k(z_0 - z_i)$, cal/cm^2-sec.)

3

l length of telescope tube (mirror to opening), radii

m   distance from mirror to beginning of heated isothermal collar, radii

n   distance from mirror to end of heated isothermal collar, radii

p   half the spacing between circumferential heat pipes, cm

p,q,r   coefficients in power series for $z(x)$

$q = \sigma T^4$ on heated isothermal collar

r   radius of cylinder, cm

s   factor for radiation exchange on inner wall of finite-length tube

T   temperature, K

$\overline{T}$ circumferential root mean fourth power of wall temperature, $\left(\dfrac{a_0}{\sigma}\right)^{1/4}$, K

t   time, sec

u   rate at which radiation leaves a unit area, cal/cm^2-sec

x   longitudinal distance along tube from mirror, radii

x   longitudinal distance from circle midway between adjacent heat pipes, cm

$y = \sigma T^4$ along tube between heated isothermal collar and open end

$z = \sigma T^4$

α solar absorptivity of outside surface

θ angular distance around cylinder from subsolar point

θ' dummy variable corresponding to θ

ξ dummy variable corresponding to x

4

ρ_i reflectivity of inner cylinder wall

ϵ thermal emissivity (of outside surface unless otherwise indicated)

σ Stefan-Boltzmann constant, 1.3556×10^{-12} cal/cm^2-sec-K^4

τ wall thickness, cm

Subscripts:

o   outside surface of insulation

i   tube wall

f   finite-length tube

m   midway between circumferential heat pipes

max   maximum around circle

min   minimum around circle

1   outside surface of variant section (see sketch (j))

0,1,2,...,9   ten sheets of a multilayer insulation (eq. (34)); 9 refers to sheet adjacent to tube wall, 0 refers to outside sheet

10   tube wall

Primes denote differentiation with respect to x.

INFINITELY LONG CYLINDER

As a first step, the case of the infinitely long thin-walled metal cylinder will be analyzed. The cylinder is in space, at one astronomical unit (1 A.U.) from the sun, with its axis normal to the solar radiation. No other radiation is present, so only the sunlit half receives radiation, while the other half receives no radiation at all.

The following section will consider the simple case of the uninsulated cylinder in order to exemplify the method of analysis. Subsequent sections will consider the effects

of (1) insulation, (2) circumferential heat conduction in the cylinder wall, and (3) circum-ferential heat pipes attached to the cylinder wall. The analysis is similar in many respects to that of reference 5.

Uninsulated Cylinder

Internal radiation exchange.- The inner surface of the cylinder is assumed to be perfectly black. Then, of the radiation emitted from any (infinitely long) longitu-dinal element of the internal surface at θ', the fraction $\frac{1}{4} \sin \frac{|\theta' - \theta|}{2} d\theta$ is received by an element at θ of angular width $d\theta$ (ref. 6, pp. 19-21). (See sketch (b).)
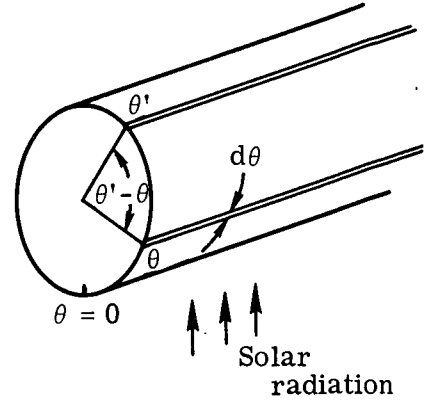
The basic variable will be taken, not as tempera-ture T, but as $z \equiv \sigma T^4$, where σ is the Stefan-Boltzmann constant. Let the distribution of z around the cylinder be given by a cosine series in θ, the angle from the subsolar point:

Sketch (b)

$$z(\theta) \equiv \sigma T^4(\theta) = a_0 + a_1 \cos \theta + a_2 \cos 2\theta + a_3 \cos 3\theta + \ldots \tag{1}$$

Then at any circumferential location θ, the received radiation intensity contributed by the $\cos n\theta$ term is

$$\frac{1}{4} a_n \int_{\theta'=\theta}^{\theta+2\pi} \cos n\theta' \sin \frac{\theta' - \theta}{2} d\theta' = - \frac{a_n}{4n^2 - 1} \cos n\theta \tag{2}$$

Thus, the received radiation intensity also varies as $\cos n\theta$, but its phase is reversed and its amplitude is reduced by the factor $4n^2 - 1$.

Temperature distribution.- Let the cylinder diameter be so large relative to the wall thickness (for example, a 3-meter-diameter cylinder with a wall of 1-mm-thick aluminum) that heat transfer by thermal conduction around the wall is negligible in com-parison with heat transfer by radiation across the inside of the cylinder.

Let

b   solar constant, $\frac{1}{30}$ cal/cm^2-sec

α solar absorptivity of external surface

ϵ thermal emissivity of external surface

6

As already noted, the internal surface is assumed to be a perfect absorber and emitter. Then, on the sunlit half of the cylinder $\left(|\theta| < \frac{\pi}{2}\right)$,

$$\alpha b \cos \theta - \sum_{n=0}^{\infty} \frac{a_n}{4n^2 - 1} \cos n\theta = (1 + \epsilon) \sum_{n=0}^{\infty} a_n \cos n\theta \qquad \left(|\theta| < \frac{\pi}{2}\right) \qquad (3)$$

where the first term on the left is the heat input from the sun; the second term on the left is the heat received by radiation from the entire internal surface of the cylinder (see eq. (2)); the term $\epsilon \sum a_n \cos n\theta$ on the right is the heat radiated away from the outer surface; and the remaining term on the right, $\sum a_n \cos n\theta$, is the heat radiated from the inner surface.

For the shaded half of the cylinder $\left(\frac{\pi}{2} < |\theta| < \pi\right)$, the first term on the left-hand side of equation (3) is omitted, and the equation becomes

$$-\sum_{0}^{\infty} \frac{a_n}{4n^2 - 1} \cos n\theta = (1 + \epsilon) \sum_{0}^{\infty} a_n \cos n\theta \qquad \left(\frac{\pi}{2} < |\theta| < \pi\right) \qquad (4)$$

Equations (3) and (4) may be combined by introducing the function $\cos^* \theta$, which is the same as $\cos \theta$ for $|\theta| < \frac{\pi}{2}$ and which is zero for $\frac{\pi}{2} < |\theta| < \pi$. (See sketch (c).) The combined equation is

Sketch (c)
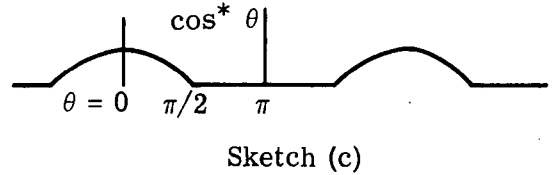
$$\alpha b \cos^* \theta - \sum_{0}^{\infty} \frac{a_n}{4n^2 - 1} \cos n\theta = (1 + \epsilon) \sum_{0}^{\infty} a_n \cos n\theta \qquad \left(0 < |\theta| < \pi\right)\cdot \qquad (5)$$

The function $\cos^* \theta$ may be expanded in a Fourier series:

$$\cos^* \theta = \frac{1}{\pi} + \frac{\cos \theta}{2} + \frac{2}{3\pi} \cos 2\theta - \frac{2}{15\pi} \cos 4\theta + \frac{2}{35\pi} \cos 6\theta - \ldots$$

$$+ (-1)^{\frac{n}{2}-1} \frac{2 \cos n\theta}{\left(n^2 - 1\right)\pi} \theta \qquad \qquad (n \text{ even}) \qquad (6)$$

Substituting this series for $\cos^* \theta$ in equation (5) gives

$$\alpha b \left(\frac{1}{\pi} + \frac{\cos \theta}{2} + \frac{2}{3\pi} \cos 2\theta - \ldots\right) = \sum_{0}^{\infty} \left(\frac{1}{4n^2 - 1} + 1 + \epsilon\right) a_n \cos n\theta \qquad (7)$$

7

The a_n are now found from this equation simply by equating coefficients of $\cos n\theta$. The results are

$$a_0 = \frac{\alpha b}{\pi \epsilon}$$

$$a_1 = \frac{\alpha b}{2\left(\frac{4}{3} + \epsilon\right)}$$

$$a_2 = \frac{2\alpha b}{3\pi\left(\frac{16}{15} + \epsilon\right)}$$

$$a_4 = -\frac{2\alpha b}{15\pi\left(\frac{64}{63} + \epsilon\right)}$$

$$a_6 = \frac{2\alpha b}{35\pi\left(\frac{144}{143} + \epsilon\right)}$$

$$\vdots \qquad \vdots$$

$$a_n = (-1)^{\frac{n}{2}-1} \frac{2\alpha b}{\left(n^2 - 1\right)\pi\left(\frac{4n^2}{4n^2 - 1} + \epsilon\right)} \qquad \text{(n even)}$$

$$a_3 = a_5 = a_7 = \ldots = 0$$

$$\left.\begin{array}{c}\\\\\\\\\\\\\\\\\\\\\\\\\\\end{array}\right\} \quad (8)$$

With these coefficients, the series (1) may be evaluated to give $\sigma T^4(\theta)$, from which $T(\theta)$ may be determined. The constant term of the series, a_0, which is the circumferential average value of σT^4, depends only on the α/ϵ ratio, and not on the separate values of α and ϵ.

Figure 1 shows the calculated circumferential temperature distributions for the following four pairs of values of external absorptivity and emissivity:

Case	α	ϵ
1	1.0	1.0
2	.4	.4
3	.25	.85
4	.15	.85

8

The third and fourth cases correspond roughly to white paints. (One might also consider the fourth to represent a fresh white paint, and the third to represent the same paint after extended exposure in space.) The second case might correspond roughly to a metallic paint, like fine aluminum flake in a suitable clear vehicle. The first case, of course, corresponds to a theoretically black surface.

The root mean fourth power of the temperature $(a_0/\sigma)^{1/4}$, designated as $\overline{T}$, has been indicated by a short line for each case. Its value is somewhat higher than the true average temperature.

The curves have about the expected shapes, but several features might be mentioned:

(1) The coolest part of the wall is not at the antisolar point, $\theta = 180^{\circ}$, but at $\theta = 90^{\circ}$. The reason is that the hot subsolar area around $\theta = 0^{\circ}$ radiates more strongly to the antisolar point than to any other point, because of the $\sin\frac{|\theta' - \theta|}{2}$ factor, which is a maximum when $|\theta' - \theta| = 180^{\circ}$; whereas a point just at the edge of the shadow receives the least radiation. As will be shown subsequently, circumferential heat conduction in the wall will eliminate the sharp breaks in the curves at $\theta = \frac{\pi}{2}$ and will also shift the location of the temperature minimum to larger angles.

(2) The curves all seem to pass through $\overline{T}$ near $\theta = 70^{\circ}$.

(3) Although cases (1) and (2) have the same value of α/ϵ, the first shows a much larger temperature variation than the second. The reason is that the temperature-equalizing tendency of the internal radiation exchange is the same in both cases (since the internal surface was assumed to be black), and is thus relatively more important in the second case, where the external heat exchange is weaker (that is, lower α and ϵ) than in the first case.

(4) The largest temperature difference between the warmest and coolest points is 99 K (for $\alpha = \epsilon = 1.0$); and the smallest temperature difference is 58 K (for $\alpha = 0.15$; $\epsilon = 0.85$). Differences of this order are unacceptable for the telescope. It is apparent that a very effective insulation will be essential in order for the rate of heat flow between the outside and the inside to be very small relative to the rate of heat exchange by radiation within the cylinder.

The effect of a gray internal surface.- In the preceding analysis the internal surface was assumed to be perfectly black, for which case the fraction of the radiation emitted from an element at θ' that is received by an element of angular width $d\theta$ at location θ is $\frac{1}{4}\sin\frac{|\theta' - \theta|}{2}d\theta$. If the internal emissivity is some value $\epsilon_i < 1$, not only is the emitted radiation reduced by the factor ϵ_i (for given $T(\theta')$), but the fraction of this radiation that is absorbed by the element at θ (including what is absorbed after one or more reflections) is changed to

$$\frac{\epsilon_i^{1/2} \cos\left\{\epsilon_i^{1/2} \dfrac{\left[\pi - (\theta' - \theta)\right]}{2}\right\}}{4 \sin\left(\epsilon_i^{1/2} \dfrac{\pi}{2}\right)} \, d\theta$$

(See ref. 7; a related analysis is given in ref. 8.) For ϵ_i values of about 0.90 to 0.95, the value of this expression is less than $\dfrac{1}{4} \sin \dfrac{|\theta' - \theta|}{2}$ for $|\theta' - \theta| > 81^\circ$, and exceeds it for $|\theta' - \theta| < 81^\circ$.

Correspondingly, equation (2) for the absorbed radiation intensity contributed by the $\cos n\theta$ term is changed to

$$\epsilon_i a_n \int_{\theta'=\theta}^{\theta+2\pi} \cos n\theta' \; \frac{\epsilon_i^{1/2} \cos\left\{\epsilon_i^{1/2} \dfrac{\left[\pi - (\theta' - \theta)\right]}{2}\right\}}{4 \sin\left(\epsilon_i^{1/2} \dfrac{\pi}{2}\right)} \, d\theta' = -\frac{\epsilon_i^2}{4n^2 - \epsilon_i} a_n \cos n\theta$$

If the factor $\dfrac{\epsilon_i^2}{4n^2 - \epsilon_i}$ is substituted for $\dfrac{1}{4n^2 - 1}$ in equation (7), the Fourier coefficients (eqs. (8)) become

$$\left.\begin{aligned}
a_0 &= \frac{\alpha b}{\pi \epsilon_o} \\[2em]
a_1 &= \frac{\alpha b}{2\left(\dfrac{4\epsilon_i}{4 - \epsilon_i} + \epsilon_o\right)} \\
&\quad \vdots \qquad \vdots \\[1em]
a_n &= (-1)^{\frac{n}{2}-1} \frac{2\alpha b}{\left(n^2 - 1\right)\pi \left(\dfrac{4n^2 \epsilon_i}{4n^2 - \epsilon_i} + \epsilon_o\right)} \qquad \text{(n even)} \\[2em]
a_3 &= a_5 = a_7 \ldots = 0
\end{aligned}\right\} \qquad \text{(8a)}$$

where the outside emissivity has been written ϵ_o to distinguish it from the internal emissivity ϵ_i.

Values of ϵ_i of about 0.95 have been reported for some mat black coatings such as would presumably be used in the telescope tube. With such values, the temperature variation around the tube would be increased (relative to what is shown in fig. 1) by

10

about 5 percent. Accordingly, the results shown in the present paper, which are all based on $\epsilon_i = 1$, slightly underestimate the circumferential temperature variation.

The Effect of Insulation

Assumed insulation characteristics.- Consider the cylinder to be wrapped in multilayer insulation – that is, many layers of aluminized plastic sheet, loosely packed. The multilayer insulation is idealized in the sense that heat transfer across it will be assumed to occur only by radiation between adjacent layers. Such idealization provides important simplification of the analysis because it permits $z(\equiv \sigma T^4)$ to be retained as the basic variable in all parts of the analysis; in particular, the heat flow through the insulation is proportional to the difference between the z values on the outer and inner surfaces. Thus, the heat flow is written as $k(z_o - z_i)$, where k is a "radiation conductance," z_o is the value of z on the outermost layer of insulation, and z_i is the value of z on the inner cylinder. For a small difference between the temperatures T_o and T_i, the heat flow would then be

$$k\Delta\left(\sigma T^4\right) \approx 4k\sigma T^3 \Delta T$$

where the factor $4k\sigma T^3$ may be interpreted as the usual conductance, which, however, varies rapidly with T.

In order to test the approximate validity of this concept, one might examine whether measured conductivities of multilayer insulations do indeed vary with T^3. In references 9 and 10 (p. 10) are a set of data for several different multilayer insulations, obtained with a very sensitive apparatus that could provide conductivity values even when ΔT was as small as 6 K. These data have been replotted on a log-log plot in figure 2. Best-fit straight lines are shown for the various insulations; in addition, an exact T^3 variation (the heavy solid line) has been added to the plot. It will be seen, first, that most of the groups of data points do indeed lie nearly on straight lines; and furthermore it will be seen that the slopes of most of the lines lie between 2 and 3, whereas two of the lines have slopes exceeding 3 (3.5 and 4.25). The high slopes are not necessarily in error, since theory predicts that the aluminum coatings should have an emissivity approximately proportional to T (as may be shown, for example, from eq. (2) of ref. 11, by using handbook values of the electrical resistivity of pure aluminum), which would cause the conductivities to vary as T^4 rather than as T^3. The lines with the smallest slopes are for the insulations with the highest packing densities, for which there is presumably an increased proportion of conductive heat transfer. On the whole, then, one may conclude from figure 2 that the T^3 variation assumed for the present analyses is not unreasonable for a well constructed multilayer insulation that is not too densely packed.

In the calculations to be presented later, k values of 0.001, 0.0025, and 0.025 were used for the insulation. Since the thermal emissivity of aluminized Mylar sheet is

about 0.05, these values correspond theoretically to about 25, 10, and 1 or 2 layers, respectively. The heavy solid line of figure 2 corresponds to a 1-cm-thick insulation for which $k = 0.0025$. Since the line lies within the range of test results, values of the order of 0.0025 may thus be considered as fairly realistic (although it is well known that careful design and construction are necessary to prevent extraneous heat flows that greatly exceed predictions from such laboratory values).

Derivation of Fourier coefficients.- The problem is set up as before, although it is now slightly more complicated. On the sunlit half of the cylinder, the heat flow through the insulation satisfies the equation

$$\alpha b \cos \theta = \epsilon z_0 + k\left(z_0 - z_i\right) \qquad \left(|\theta| < \frac{\pi}{2}\right) \qquad (9)$$

where the left-hand side of the equation is the solar heat input to the outermost sheet of insulation; the first term on the right is the heat radiated to space from this outermost sheet; and the second term on the right is the heat transferred through the insulation from the outermost sheet to the inner cylinder. The z terms are functions of θ. On the shaded half of the cylinder, the solar heat input is zero, and the equation is

$$0 = \epsilon z_0 + k\left(z_0 - z_i\right) \qquad \left(\frac{\pi}{2} < |\theta| < \pi\right) \qquad (10)$$

Equations (9) and (10) may be combined, as before, by writing

$$\alpha b \cos^* \theta = \epsilon z_0 + k\left(z_0 - z_i\right) \qquad (11)$$

Solving for z_0 gives

$$z_0 = \frac{\alpha b \cos^* \theta + k z_i}{\epsilon + k}$$

whence

$$z_0 - z_i = \frac{\alpha b \cos^* \theta - \epsilon z_i}{\epsilon + k} \qquad (12)$$

Equilibrium of the inner cylinder provides the equation

$$k\left(z_0 - z_i\right) - \sum_0^\infty \frac{a_n}{4n^2 - 1} \cos n\theta = \sum_0^\infty a_n \cos n\theta \qquad (13)$$

where the first term on the left is the heat transferred in through the insulation at θ, the second term on the left is the radiation received at θ from the entire inner surface of the cylinder, and the term on the right is the heat radiated away from the element at θ into the inside of the cylinder. Substituting the expression for $z_0 - z_i$ from equation (12) into equation (13), while replacing $\cos^* \theta$ with its Fourier series and replacing z_i with $\sum_0^\infty a_n \cos n\theta$, gives

12

$$\frac{k\alpha b}{\epsilon + k}\left(\frac{1}{\pi} + \frac{\cos\theta}{2} + \frac{2}{3\pi}\cos 2\theta - \ldots\right) = \sum_{0}^{\infty}\left(\frac{\epsilon k}{\epsilon + k} + \frac{1}{4n^2 - 1} + 1\right)a_n \cos n\theta$$

from which, by equating coefficients of $\cos n\theta$, the Fourier coefficients for z_i are obtained:

$$\left.\begin{array}{l} a_0 = \dfrac{\alpha b}{\pi \epsilon} \\[3mm] a_1 = \dfrac{\alpha b}{2\left(\dfrac{4}{3}\dfrac{\epsilon + k}{k} + \epsilon\right)} \\[5mm] a_2 = \dfrac{2\alpha b}{3\pi\left(\dfrac{16}{15}\dfrac{\epsilon + k}{k} + \epsilon\right)} \\[5mm] \quad\vdots \qquad\qquad \vdots \end{array}\right\} \tag{14}$$

The coefficient a_0 (the average value of z_i) is the same as before. The other coefficients are changed only by the factor $(\epsilon + k)/k$ on one of the terms in the denominator. With $k = \infty$, the coefficients reduce to those previously derived for the uninsulated cylinder (eq. (8)).

The Effect of Circumferential Heat Conduction

It was previously indicated that for the Large Space Telescope, the heat conduction around the cylinder would be negligible relative to the radiation heat transfer. It would not be negligible for a much smaller telescope, however; so, for completeness, the preceding analysis will be extended to include this effect. The equations will be developed for the general case in which the wall thickness is τ cm and the conductivity of the wall material is C cal/cm-sec-K. In all the computed examples, however, the wall will be assumed to be 0.1-cm-thick aluminum ($\tau = 0.1$; $C = 0.5$; $C\tau = 0.05$).

The circumferential flow of heat, by conduction, into 1 cm^2 of the wall is $C\tau\dfrac{d^2T}{r^2 d\theta^2}$, where r is the cylinder radius. With $z_i = \sigma T^4$, $\dfrac{dz_i}{d\theta} = 4\sigma T^3\dfrac{dT}{d\theta}$, or, since T remains close to its root mean fourth power $\overline{T}$,

$$\frac{dz_i}{d\theta} \approx 4\sigma\overline{T}^3\frac{dT}{d\theta}$$

$$\frac{d^2z_i}{d\theta^2} \approx 4\sigma\overline{T}^3\frac{d^2T}{d\theta^2}$$

13

Since $\sigma\overline{T}^4 = a_0$ (the constant term in the Fourier series for z_i), the factor $4\sigma\overline{T}^3 = \dfrac{4a_0}{(a_0/\sigma)^{1/4}} = 4\sigma^{1/4}a_0^{3/4}$. The conduction term $C\tau\dfrac{d^2T}{r^2 d\theta^2}$ thus reduces to

$$\frac{C\tau}{4r^2\sigma^{1/4}a_0^{3/4}}\frac{d^2z_i}{d\theta^2} = -\frac{C\tau}{4r^2\sigma^{1/4}a_0^{3/4}}\sum_1^\infty n^2 a_n \cos n\theta$$

(where the series in eq. (1) has been substituted for z_i). This term is now inserted into the left-hand side of equation (13) as an additional heat-input term. The Fourier coefficients for the insulated cylinder, with circumferential conduction taken into account, are now found as

$$\left.\begin{aligned}
a_0 &= \frac{\alpha b}{\pi\epsilon} \\[2em]
a_1 &= \frac{\dfrac{k\alpha b}{\epsilon + k}}{2\left(\dfrac{4}{3} + \dfrac{\epsilon k}{\epsilon + k} + \dfrac{C\tau}{4r^2\sigma^{1/4}a_0^{3/4}}\right)} \\[2em]
&\ \ \vdots \qquad\qquad\qquad \vdots \\[2em]
a_n &= (-1)^{\frac{n}{2}-1}\frac{\dfrac{2k\alpha b}{\epsilon + k}}{\left(n^2 - 1\right)\pi\left(\dfrac{4n^2}{4n^2 - 1} + \dfrac{\epsilon k}{\epsilon + k} + \dfrac{C\tau n^2}{4r^2\sigma^{1/4}a_0^{3/4}}\right)} \quad (n \ \ \text{even}) \\[2em]
a_3 &= a_5 = a_7 = \ldots = 0
\end{aligned}\right\} \tag{15}$$

Calculated results will be presented after the following section.

### The Effect of Circumferential Heat Pipes

Derivation of heat-transfer term.- Suppose that the infinite cylinder has circumferential heat pipes around it at small fixed intervals. (See sketch (d).) These pipes would serve to reduce the circumferential temperature variation. For the present analysis it will be assumed that the heat pipes are perfect conductors and that the technique of bonding them to the wall provides negligible thermal resistance between the pipes and the wall. They thus provide a periodic distribution of isothermal rings along the cylinder. Admittedly, present technology frequently produces only a poor approximation to the
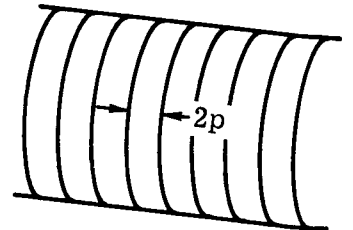
Sketch (d)

assumed ideal conditions. However, it may be hoped that the present research and development effort in this field will result in significant advances in the art during the next few years.

The heat pipes acquire the average temperature of the cylinder. For most of the sunlit half, heat is delivered to the heat pipes, flowing along the wall toward them; and in the shaded half, heat is removed from the heat pipes, flowing along the wall away from them. Correspondingly, along any longitudinal cylinder element there will be a periodic variation of temperature, about as shown in sketch (e). The short arcs in the sketch are
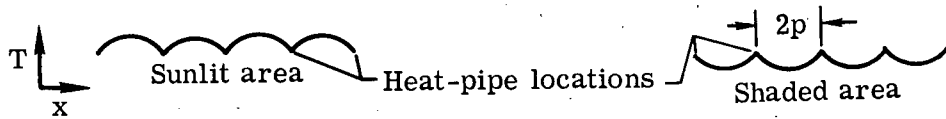
Sketch (e)

approximately parabolic. (In the one-dimensional case with uniform addition or loss of heat by radiation, the governing differential equation is $\dfrac{d^2T}{dx^2}$ = Constant, for which the variation of T with x would be exactly parabolic.)

Two modifications to the analysis result:

(1) Corresponding to the longitudinal heat flow in the wall, the rate of loss of heat from a cm^2 of wall is $-C\tau\dfrac{\partial^2 T}{\partial x^2}$, where, as before, the factor $C\tau$ is the product of wall thickness (τ cm) and conductivity (C cal/cm-sec-K). The parabolic variation gives

$$\Delta T = (\Delta T)_m\left[1 - \left(\frac{x}{p}\right)^2\right]$$

from which

$$\frac{\partial^2 T}{\partial x^2} = -\frac{2(\Delta T)_m}{p^2}$$

where

p   half the spacing between heat pipes

ΔT wall temperature minus heat-pipe temperature

ΔT_m value of ΔT midway between adjacent heat pipes

x   longitudinal distance from midway point, cm

15

Since the range of variation of T is small, the parabolic distribution of T implies a parabolic distribution of z $\left(= \sigma T^4\right)$ also. Let $z_i = a_0 + \sum_1^\infty a_n \cos n\theta$ be σT^4 on the circle that is midway between adjacent heat pipes, where a_0, the average value of z_i, is also the heat pipe value of σT^4. Then ΔT_m corresponds to $\sum_1^\infty a_n \cos n\theta$; or, by the relationship derived in the preceding section,

$$\Delta T_m = \frac{\Delta z_m}{4\sigma \overline{T}^3} = \frac{1}{4\sigma^{1/4} a_0^{3/4}} \sum_1^\infty a_n \cos n\theta$$

The conduction heat flow out of the wall toward the heat pipes, per cm^2, is then

$$-C\tau \frac{\partial^2 T}{\partial x^2} = -C\tau\left(\frac{-2\,\Delta T_m}{p^2}\right) = \frac{C\tau}{2p^2\sigma^{1/4} a_0^{3/4}} \sum_1^\infty a_n \cos n\theta$$

(2) Since the average height of a parabolic arc is two-thirds of its maximum height (sketch (f)), the average z along any infinite longitudinal element is $a_0 + \frac{2}{3}\sum_1^\infty a_n \cos n\theta$.

This average value will be used in the term for the radiation received at θ from the inside of the cylinder (a modification of eq. (2)).

Sketch (f)
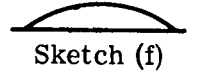
It must be noted that the assumed fairly small heat pipe spacing is necessary for the preceding discussion to be valid. For example, if the spacing is very large, the longitudinal temperature distribution would no longer be approximately parabolic, so that neither the two-thirds factor nor the expression for $\partial^2 T/\partial x^2$ would be valid.

Heat-balance equation and solution.- The heat-balance equation, including the terms for insulation, circumferential conduction, and longitudinal conduction to heat pipes, is, for the circle that is midway between adjacent heat pipes,

$$k(z_0 - z_i) + a_0 - \frac{2}{3} \sum_1^\infty \frac{1}{4n^2 - 1} a_n \cos n\theta$$

$$= a_0 + \sum_1^\infty a_n \cos n\theta + \frac{C\tau}{4r^2\sigma^{1/4} a_0^{3/4}} \sum_1^\infty n^2 a_n \cos n\theta + \frac{C\tau}{2p^2\sigma^{1/4} a_0^{3/4}} \sum_1^\infty a_n \cos n\theta \qquad (16)$$

where the first term on the left is the heat transmitted in through the insulation; the second and third terms on the left represent the radiation received from the inside of the cylinder; the first two terms on the right represent the heat radiated away into the inside of the cylinder; the third term on the right is the heat conducted away circumferentially; and the fourth term on the right is the heat conducted away longitudinally.

16

As before, the factor $(z_0 - z_i)$ is replaced by the expression in equation (12); and the Fourier coefficients are then determined by the procedure previously described. They are

$$a_0 = \frac{\alpha b}{\pi \epsilon}$$

$$a_1 = \frac{\dfrac{k\alpha b}{k + \epsilon}}{2\left(1 + \dfrac{2}{3 \times 3} + \dfrac{k\epsilon}{k + \epsilon} + \dfrac{C\tau}{4r^2 \sigma^{1/4} a_0^{3/4}} + \dfrac{C\tau}{2p^2 \sigma^{1/4} a_0^{3/4}}\right)}$$

$$a_2 = \frac{2\dfrac{k\alpha b}{k + \epsilon}}{3\pi\left(1 + \dfrac{2}{3 \times 15} + \dfrac{k\epsilon}{k + \epsilon} + \dfrac{4C\tau}{4r^2 \sigma^{1/4} a_0^{3/4}} + \dfrac{C\tau}{2p^2 \sigma^{1/4} a_0^{3/4}}\right)}$$

$$\vdots \qquad\qquad \vdots$$

$$a_n = (-1)^{\frac{n}{2}-1} \frac{2\dfrac{k\alpha b}{k + \epsilon}}{(n^2 - 1)\pi\left[1 + \dfrac{2}{3(4n^2 - 1)} + \dfrac{k\epsilon}{k + \epsilon} + \dfrac{n^2 C\tau}{4r^2 \sigma^{1/4} a_0^{3/4}} + \dfrac{C\tau}{2p^2 \sigma^{1/4} a_0^{3/4}}\right]}$$

$$\text{(n even)}$$

$$a_3 = a_5 = a_7 = \ldots = 0$$

$$\left.\rule{0pt}{12em}\right\} \quad (17)$$

These coefficients reduce to those for the case without heat pipes (coefficients (15)) if the last term in the brackets is deleted and if the factor 2/3 is changed to 1. If the fourth term in the brackets is also deleted, the coefficients (14) are obtained. Finally, if k is made infinite, the coefficients (8) are obtained.

Calculated Results

A number of circumferential temperature distributions were calculated by means of the sets of Fourier coefficients (14), (15), and (17). As previously mentioned, for all cases in which heat conduction in the wall was considered, the product of wall thickness and conductivity was taken as 0.05.

The cylinder radius r was taken as 150 cm for most of the calculations, but a few calculations were made for a radius of 15 cm. The effect of circumferential conduction (given by the term containing r in the coefficients (15) and (17)) is not important for r = 150 cm; but since r occurs as the inverse square, the effect rapidly increases in

importance as r decreases. The heat-pipe spacing 2p was taken as 40 cm for all heat-pipe calculations. The isothermalizing effect of heat pipes also varies inversely as the square, as indicated by the p^2 factor in the last term in the brackets in the coefficients (17).

Figure 3 shows circumferential temperature distributions calculated with circumferential conduction taken into account. The cylinder radius was taken as 150 cm for all cases but one. For the insulation, k values of 0.001, 0.0025, 0.025, and ∞ were used (k = ∞ corresponds to no insulation). In figure 3(a), for k = ∞, a curve from the zero-conduction results of figure 1 has been added (the dashed curve). It is seen that the circumferential conduction has relatively little effect for a large cylinder (r = 150 cm), although it does serve to wash out the break at $\theta = 90^o$. On the other hand, when r is only 15 cm, the temperature-equalizing effect of conduction is seen to be very pronounced, since the circumferential variation is now only half as much as when r = 150 cm.

Comparison of the curves in figure 3(a) with the upper set in figure 3(b) shows that even a little insulation will greatly increase the temperature uniformity. For k = 0.025, corresponding to only one or two layers of aluminized plastic sheet, the variation was reduced by a factor of about 15. For k = 0.0025, the variation is only a few tenths of a degree.

Comparison of the three sets of curves in figure 3(b) shows that for a given α and ϵ, the temperature variations are approximately proportional to k. In fact, for the two smallest values of k (the lower two sets of curves), the proportionality to k is almost exact.

The curves in figure 4 show the further improvement in temperature uniformity that can be obtained with heat pipes. The upper set of curves, for the zero-insulation case, shows improvements by factors of 1.9 to 3.3, compared with the curves of figure 3(a). The lower set, for k = 0.0025, shows improvements by factors of 2.3 to 5.7. As already indicated, reducing the heat-pipe spacing would cause rapid further improvement. It must also be noted that these results in figure 4 are for the circle midway between adjacent heat pipes. The average variation around the cylinder is only about two-thirds as much.

Calculations were also made for k = 0.025 and 0.001 for the heat-pipe case. The results are not shown, since the curves are again simply proportional to k, and may be derived from the results shown in figure 4 for k = 0.0025.

The quantities of heat transported along the heat pipes turn out to be very small. For example, for the middle curve of figure 4(b) ($\alpha = 0.25$, $\epsilon = 0.85$, k = 0.0025, $\Delta T_m = 0.052$ K), the heat delivered to each heat pipe between $\theta = 0^o$ and $\theta = 70^o$ (and withdrawn from each heat pipe between $\theta = 70^o$ and $\theta = 180^o$) is only 0.061 cal/sec.

18

Accordingly, the original assumption that the heat pipes are essentially isothermal seems to be justified. The other assumption — that the bonding between the heat pipes and the wall has negligible thermal resistance — seems, with present technology, to be more questionable.

FINITE-LENGTH CYLINDER

The preceding analyses of the infinitely long cylinder show how to calculate the degree of <u>circumferential</u> temperature nonuniformity for given wall, insulation, thermal coating, and heat-pipe spacing. The present section will consider the <u>longitudinal</u> temperature variation along a cylinder of finite length. It will be first assumed that, by means of insulation and heat pipes, the circumferential temperature variation has been made negligibly small or, at least, has been made so small that it can be considered independently of the longitudinal temperature variation. That is, the internal wall temperature will be considered as a function of longitudinal location only. Some discussion and analyses of circumferential temperature variation will be given later.

Since circumferential heat flow is not considered for the present, it will be convenient, in the analysis, to take the cylinder radius as unity.

Net Heat Flow Through the Insulation

In the preceding analyses the average value a_0 of σT^4, either outside or inside the infinite cylinder, was $\alpha b / \pi \epsilon$. In a finite-length cylinder, the internal σT^4 is everywhere less than this value because heat is lost by radiation out of the open end. Correspondingly, the average external σT^4 at any longitudinal location is less than $\alpha b / \pi \epsilon$, because the outside is the source of this lost heat and is continuously supplying it through the insulation. The symbol a_0 will be retained, for the present, for $\alpha b / \pi \epsilon$, and the symbol a will be used to represent the local circumferential average σT^4 of the outermost layer of insulation. The local circumferential average σT^4 of the cylinder wall will be designated z.

It is apparent that the local rate of heat supply through the insulation is proportional to $a - z$. However, it is also proportional to $a_0 - z$. The proof follows: At any given longitudinal location along the (unit-radius) tube, the heat-flow equation for a circular band 1 cm wide is

$$2\alpha b = 2\pi a \epsilon + 2\pi (a - z)k$$

where the left-hand side represents the rate of absorption of solar heat by the outer layer of insulation; the first term on the right is the rate of radiation of heat away from the outer layer; and the last term is the rate of transfer of heat through the insulation to the inner cylinder wall. Solving for a gives

$$a = \frac{\alpha b + \pi kz}{\pi(k + \epsilon)}$$

Substituting this expression for a in the term $2\pi k(a - z)$, which is the rate of heat transfer in through the insulation, gives

$$2\pi k(a - z) = 2\pi k\left[\frac{\alpha b + \pi kz}{\pi(k + \epsilon)} - z\right]$$

$$= 2\pi k\left[\frac{\alpha b - \pi \epsilon z}{\pi(k + \epsilon)}\right]$$

$$= \frac{2\pi k\epsilon}{k + \epsilon}\left(\frac{\alpha b}{\pi \epsilon} - z\right)$$

$$= 2\pi c\left(a_0 - z\right) \tag{18}$$

where c is $\frac{k\epsilon}{k + \epsilon}$. Thus, the rate of heat transfer in through the insulation is proportional to $a_0 - z$, as was to be proved. The product $c(a_0 - z)$ is the average heat transferred in per unit area at that location, and will be used in this form in the subsequent analyses.

The Exponential View Factor

Given a unit-radius cylinder (sketch (g)) with its inner surface perfectly black, and given two elemental circular bands of this surface, one at the origin, the other at x, the fraction of the total radiation emitted from the first band that is transmitted to the second band, per unit width of the second band, is (ref. 12)

$$\frac{1}{2}\left[1 - \frac{|x|(x^2 + 6)}{(x^2 + 4)^{3/2}}\right]$$

Sketch (g)
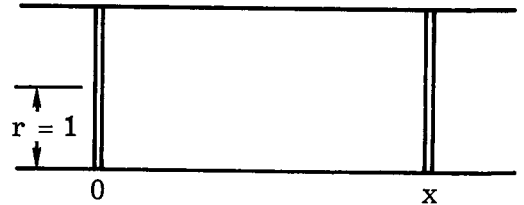
It was shown in reference 12 that this view factor is roughly approximated by the simple exponential expression $\frac{1}{2}e^{-|x|}$; and that use of the exponential expression greatly simplifies the analysis of radiation exchange within a cylinder.

The two functions are compared in figure 5. The areas under the two curves are the same. The expressions have the same values at $|x| = 0$, 1.106, 4.608, and ∞. At large $|x|$, the exponential curve lies below that for the perfect radiator. One might hence argue that the exponential curve is the more representative of actual mat black finishes,

20

which tend to become reflectors for radiation received at glancing angles. On the other hand, the exponential curve lies above the curve for the perfect radiator for x between 1.106 and 4.608, and hence, in this respect, it represents a thermodynamically impossible surface finish. Of course, if the exponential curve is uniformly lowered by an emissivity factor of, say, 0.85, it would lie nearly completely below the curve for the perfect radiator, so that this objection would not apply. However, 0.85 is considerably below the emissivities of available black finishes. A better approach might be to use a sum of two or three exponentials $\left(\text{for example, } 0.605e^{-1.14|x|} - 0.105e^{-3.42|x|}\right)$ to provide a better approximation to the curve for the perfect radiator, as was suggested in references 12 to 15. The mathematics remains tractable, although, of course, it becomes much more cumbersome. However, the slightly improved analytical accuracy attainable with such modifications would have little practical significance for the present study and would not justify the greatly increased computational effort. Accordingly, the simple exponential view factor $\frac{1}{2}e^{-|x|}$ will be used in the present analyses. Some additional analytical justification, other than the similarity of the two curves of figure 5, will be given later. A practical consideration is simply that the paint and insulation characteristics would not be so accurately known or so accurately uniform and reproducible that extreme effort to achieve analytical accuracy is warranted. Furthermore, since the assumed configuration does not take into account the presence of the secondary mirror and its supporting structure, the curvature of the primary mirror, or the hole in its center, it would hardly be reasonable to insist on ultimate accuracy in the analysis.

The Simple Open Tube

Consider an insulated, open-ended, internally black tube of unit radius and length $2l$, with its axis normal to the solar rays. (See sketch (h).) For present purposes, it

$$x = -l \qquad x = 0 \qquad x = l$$
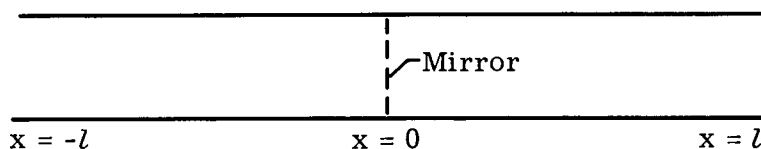
Sketch (h)

represents an idealized telescope tube of length l with a perfect flat mirror at one end ($x = 0$). The mirror reflects the inside of the tube and thus, in effect, provides for the analysis a tube of length $2l$ with both ends open.

Use of the exponential view factor provides the following integral equation for the heat balance of a unit area at any longitudinal location x:

$$z(x) = c\left[a_0 - z(x)\right] + \frac{1}{2}\int_{-l}^{x} z(\xi)e^{\xi-x}d\xi + \frac{1}{2}\int_{x}^{l} z(\xi)e^{x-\xi}d\xi \qquad (19)$$

where ξ is a dummy variable corresponding to x.

The term on the left represents the heat radiated away from the inner surface at x, per unit area; the first term on the right represents the heat received at x, per unit area, from the outside, through the insulation (see eq. (18)); the first integral represents the radiation received from the part of the wall that lies to the left of x; and the second integral represents the radiation received from the part of the wall that lies to the right of x.

Transfer the first term on the right to the left-hand side of the equation to get

$$(1 + c)z(x) - a_0c = \frac{1}{2}\int \cdots + \frac{1}{2}\int \cdots \qquad (19a)$$

Differentiate with respect to x to get

$$(1 + c)z'(x) = \frac{1}{2}z(x) - \frac{1}{2}\int_{-l}^{x} z(\xi)\, e^{\xi-x}d\xi - \frac{1}{2}z(x) + \frac{1}{2}\int_{x}^{l} z(\xi)\, e^{x-\xi}d\xi$$

Differentiate again to obtain

$$(1 + c)z''(x) = -\frac{1}{2}z(x) + \frac{1}{2}\int_{-l}^{x} z(\xi)\, e^{\xi-x}d\xi - \frac{1}{2}z(x) + \frac{1}{2}\int_{x}^{l} z(\xi)\, e^{x-\xi}d\xi$$

The two integrals on the right are now the same as the original ones in equation (19a); therefore, they may be replaced by the left-hand side of that equation. Thus, a differential equation is obtained:

$$(1 + c)z'' = -z + (1 + c)z - ca_0$$

which simplifies to

$$(1 + c)z'' = c(z - a_0)$$

the solution of which is

$$z = a_0 - A \cosh fx \qquad (20)$$

where $f = \sqrt{c/(1 + c)}$ and the coefficient A is to be determined. Since z is obviously symmetrical with respect to the origin, there will be no $\sinh fx$ term in the solution.

In order to determine A, substitute z from equation (20) into equation (19a) and perform the integrations for some convenient value of x — say, for $x = 0$.[1] Thus,

$$(1 + c)(a_0 - A) - a_0 c = \frac{1}{2} \int_{-l}^{0} (a_0 - A \cosh fx) e^{\xi} d\xi + \frac{1}{2} \int_{0}^{l} (a_0 - A \cosh f\xi) e^{-\xi} d\xi$$

where the two integrals are obviously equal. The integration proceeds without difficulty and provides a simple linear equation for A, the solution of which is

$$A = \frac{2a_0}{\dfrac{e^{-fl}}{1+f} + \dfrac{e^{fl}}{1-f}} \tag{21}$$

Putting this expression for A into equation (20) finally gives the equation for z as a function of the distance in radii along the cylinder x. Since $z = \sigma T^4$, the temperature T along the cylinder is then easily obtained.

Calculations were made of the temperature distribution along the cylinder for the following listed values of the basic parameters:

l: 6, 8, 12, 20 radii

α: $\left.\begin{matrix} 0.15 \\ 0.85 \end{matrix}\right\}$, $\left.\begin{matrix} 0.25 \\ 0.85 \end{matrix}\right\}$, $\left.\begin{matrix} 0.4 \\ 0.4 \end{matrix}\right\}$

ϵ:

k: 0.001, 0.0025, 0.025, ∞

In all cases the cylinder axis was assumed to be normal to the solar rays, the shaded half receiving no external radiation input at all.

The calculated results are shown in figure 6. It will be seen that for the uninsulated cylinders ($k = \infty$), the temperatures remain nearly equal to those for the infinitely long cylinders, except near the open end, where they drop sharply. For the insulated cylinders, the temperatures even at $x = 0$ (that is, at the mirror) are well below those of the corresponding infinite cylinders, and they drop steadily toward the open end.

The Effect of a Gray Internal Surface

Any real surface has an emissivity less than 1. The radiation from a surface is thus everywhere less than the local z. Furthermore, where this emitted radiation encounters some other part of the wall, it is only partly absorbed, and the remainder is reflected; and where the reflected part meets the wall it is again only partly absorbed,

---

[1] An alternative approach is to perform the integrations without giving x a particular value, and then equate coefficients. In more complicated problems, however, this approach may lead to much difficult algebra. The method here used, although perhaps less elegant, is, at least, straightforward.

with the remainder reflected; etc. Although this infinite sequence of partial absorptions and reflections would seem to greatly complicate the analysis, the problem is readily solved by the type of method indicated in reference 16. The method will be illustrated for the case of the finite-length cylinder that was treated in the preceding section.

Suppose that the internal surface has an emissivity of ϵ_i and a reflectivity of ρ_i (where $\epsilon_i + \rho_i = 1$). Two simultaneous equations are set up corresponding, respectively, to the following two statements:

(1) The rate u at which radiation leaves a unit area equals the rate at which heat enters that unit area through the insulation, plus the rate at which radiation arrives at that unit area from the rest of the internal cylinder surface.

(2) The rate u at which radiation leaves a unit area equals ϵ_i times the local z plus ρ_i times the rate at which internal radiation arrives at that unit area.

The two statements are translated into the following two equations, respectively:

$$(1) \quad u(x) = c\left[a_0 - z(x)\right] + \frac{1}{2}\int_{-l}^{x} u(\xi)\, e^{\xi-x} d\xi + \frac{1}{2}\int_{x}^{l} u(\xi)\, e^{x-\xi} d\xi \tag{22}$$

$$(2) \quad u(x) = \epsilon_i z(x) + \frac{\rho_i}{2}\int_{-l}^{x} u(\xi)\, e^{\xi-x} d\xi + \frac{\rho_i}{2}\int_{x}^{l} u(\xi)\, e^{x-\xi} d\xi \tag{23}$$

If the first equation is multiplied by ρ_i and subtracted from the second equation, the integrals cancel and a simple algebraic relation between z and u is obtained:

$$u\left(1 - \rho_i\right) = \epsilon_i z - \rho_i c\left(a_0 - z\right)$$

from which

$$z = \frac{u\epsilon_i + \rho_i c a_0}{\epsilon_i + \rho_i c} \tag{24}$$

Substituting this expression for z into equation (22) gives

$$(1 + g)u(x) - a_0 g = \frac{1}{2}\int_{-l}^{x} u(\xi)\, e^{\xi-x} d\xi + \frac{1}{2}\int_{x}^{l} u(\xi)\, e^{x-\xi} d\xi \tag{25}$$

where

$$g \equiv \frac{c\epsilon_i}{\epsilon_i + \rho_i c}$$

This equation is identical in form to equation (19a). It is solved similarly and has a similar solution:

C

$$u = a_0 - A \cosh hx \qquad (26)$$

where $h = \sqrt{g/(1 + g)}$. The coefficient A is evaluated by the same method as before:

$$A = \frac{2a_0}{\dfrac{e^{-h\mathnormal{l}}}{1 + h} + \dfrac{e^{h\mathnormal{l}}}{1 - h}}$$

Finally, substituting this derived u into equation (24) gives z, from which T can be obtained.

Some calculations were made for a finite-length cylinder having an internal surface emissivity of 0.85. The other conditions were: $\alpha = 0.25$; $\epsilon = 0.85$; $k = 0.0025, 0.025$, and ∞; $\mathnormal{l} = 8$. The results (not shown) could be compared with the results of the previous calculations (fig. 6) for the cases in which all the parameters were the same except that ϵ_i was 1. As expected, the wall temperatures were found to be slightly higher than those for $\epsilon_i = 1$. However, the differences were very small, ranging from a few tenths of a degree near $x = 0$ to a maximum of nearly 1^O at the open end. Furthermore, the emissivities of actual mat black surfaces would be considerably higher than 0.85. Accordingly, use of unit emissivity was considered to be satisfactory for present purposes.

Use of the Exact View Factor

It may be of interest to review a brief study of a different approach to solving the simple open tube: The exact view factor (see p. 20) was used in the integral equation, but $z(x)$ was represented by a three-term power series, $p + qx^2 + rx^4$. Equation (19a) is thus replaced by

$$(1 + c)\left(p + qx^2 + rx^4\right) - a_0 c = \frac{1}{2}\int_{-\mathnormal{l}}^{x}\left(p + q\xi^2 + r\xi^4\right)\left\{1 - \frac{(x - \xi)\left[(x - \xi)^2 + 6\right]}{\left[(x - \xi)^2 + 4\right]^{3/2}}\right\}d\xi + \frac{1}{2}\int_{x}^{\mathnormal{l}}\cdots$$

Integrating analytically results in an algebraic equation in p, q, r, and x. Substituting three different values of x — say, $x = 0$, $\mathnormal{l}/2$, and $\mathnormal{l}$ — gives three simultaneous linear equations for p, q, and r, the solution of which gives the power series for z. It is here supposed that the three-term series should provide a fairly accurate representation of z for a short tube, so that this method should give a fairly accurate result for such a tube.

Some calculations for a short tube ($\mathnormal{l} = 6$) showed excellent agreement with the corresponding results in figure 6. For $\mathnormal{l} = 8$, the agreement was not quite so close, with a maximum discrepancy of 1.5^O (at $x = 8$, with $\alpha = 0.25$, $\epsilon = 0.85$, and $k = 0.0025$). For still larger $\mathnormal{l}$, the disagreement became progressively worse, and the results became

physically unreasonable (as, for example, when the temperatures near x = 0 exceeded those for the infinite tube).

The three-term series is obviously inadequate to represent z(x) for the longer tubes. Although the representation could be improved by adding terms in $x^6, x^8, \ldots$, the amount of algebra would quickly become excessively cumbersome. If a very exact solution is needed, it would then be easier to get access to a large computer and use some available program for numerically solving such integral equations.

The fact that good agreement was found for the shorter tubes ($l \leqq 8$), where the three-term series is reasonably adequate, indicates that the simple exponential view factor is basically satisfactory for present purposes.

Circumferential Temperature Nonuniformity

For the infinitely long cylinder, with or without heat pipes, figures 3 and 4 showed the circumferential temperature variation for several combinations of insulations and thermal-control coatings. For a cylinder of finite length, the circumferential variation will be greater, mainly because of the reduced internal temperatures. At the reduced temperatures, the internal radiation is weaker and less effective in equalizing the internal temperatures; accordingly, the temperature difference between the subsolar area and the shaded area must increase before equilibrium is established. An additional, related reason, especially for the region near the open end, is that the radiation received from any longitudinal element of the cylinder is less than it would be if the element were infinitely long.

The following reasoning was used in estimating the increased circumferential nonuniformity: In equation (13), the term $-\sum_{n=0}^{\infty} \dfrac{a_n}{4n^2 - 1} \cos n\theta$ represents the radiation received at any θ from the entire infinite cylinder. If the cylinder is of finite length, this term would be too large, and should be reduced by some factor s. Furthermore, since the longitudinal distributions of T (or of z) along the elements of the cylinder would be very similar for all the elements, the factor s should be approximately the same for all points around the tube at the same longitudinal location; that is, it may be written as s(x). Accordingly, for the finite-length cylinder the term in the equation should be changed to $-s(x) \sum_0^{\infty} \dfrac{a_n}{4n^2 - 1} \cos n\theta$. The evaluation of s(x) from the local z(x) (the circumferential mean σT^4 given, say, by eq. (20)), and its use in estimating the circumferential temperature nonuniformity are outlined in the following sections.

Without heat pipes.- Equation (13) is modified by multiplying the summation on the the left-hand side by s, as just stated. After the term for circumferential heat conduction is added, the analysis proceeds precisely as before and yields the following Fourier coefficients, which are now functions of s (the subscript f has been used to indicate that the series is for a finite-length tube):

$$a_{0,f} = \frac{\alpha b}{\pi \left[(1 - s) \frac{\epsilon + k}{k} + \epsilon \right]}$$

$$a_{1,f} = \frac{\dfrac{k\alpha b}{\epsilon + k}}{2\left(1 + \dfrac{s}{3} + \dfrac{\epsilon k}{\epsilon + k} + \dfrac{C\tau}{4r^2 \sigma^{1/4} a_0^{3/4}}\right)}$$

$$\vdots \qquad\qquad \vdots$$

$$a_{n,f} = (-1)^{\frac{n}{2}-1} \frac{\dfrac{2k\alpha b}{\epsilon + k}}{\left(n^2 - 1\right)\pi\left(1 + \dfrac{s}{4n^2 - 1} + \dfrac{\epsilon k}{\epsilon + k} + \dfrac{n^2 C\tau}{4r^2 \sigma^{1/4} a_0^{3/4}}\right)} \qquad (n \text{ even})$$

$$a_{3,f} = a_{5,f} = a_{7,f} = \ldots = 0$$

(27)

(For s = 1, these coefficients reduce to the coefficients (14) for the infinite cylinder.) The coefficient $a_{0,f}$ is still the circumferential mean z_i $\left(\text{or } \sigma T^4\right)$, but it varies with s.

As an example of the use of these equations, suppose it is desired to find the circumferential temperature distribution at x = 8 radii on a cylinder of length l equal to 12 radii, for $\alpha = 0.25$, $\epsilon = 0.85$, and k = 0.0025. From figure 6, the mean temperature $\overline{T}$ at x = 8 is read as 128 K, from which the local mean z_i is $\sigma \times 128^4 = 3.64 \times 10^{-4}$. Putting this value equal to $a_{0,f}$ in the first of equations (27) and solving for s gives s = 0.981. With this value of s, all the other Fourier coefficients (27) may then be evaluated, whence the circumferential distribution of z_i and hence of T can be determined.

A number of circumferential distributions were calculated, but they are not presented here. Instead, the difference, $T_{max} - T_{min}$, between the maximum and minimum temperatures around the circle, as obtained from these calculated distributions, are plotted as functions of $\overline{T}$ in figure 7 for $\alpha = 0.25$, $\epsilon = 0.85$, and k = 0.025 and 0.0025. It is seen that with decreasing temperature, $T_{max} - T_{min}$ increases rapidly. Thus,

for the preceding example, with $\overline{T} = 128$ K, $T_{max} - T_{min}$ is 1.4 K, whereas for the infinite cylinder $\left(\overline{T} = 219\ K\right)$, $T_{max} - T_{min}$ is only 0.33 K. For the poorer insulation (k = 0.025), the values of $T_{max} - T_{min}$ become so large at the lower temperatures that the basic assumption (the simple modification of eq. (13)) is no longer accurate, so that the large derived values of $T_{max} - T_{min}$ must be considered as only rough approximations.

With heat pipes.- The preceding analysis can be further modified for the case of the cylinders with heat pipes. One first modifies equation (16) by multiplying the second and third terms on the left by s. The Fourier coefficients are then determined as before:

$$a_{0,f} = \frac{\alpha b}{\pi\left[(1 - s)\dfrac{\epsilon + k}{k} + \epsilon\right]}$$

$$a_{1,f} = \frac{\dfrac{k\alpha b}{\epsilon + k}}{2\left(1 + \dfrac{2s}{9} + \dfrac{\epsilon k}{\epsilon + k} + \dfrac{C\tau}{4r^2\sigma^{1/4}a_0^{3/4}} + \dfrac{C\tau}{2p^2\sigma^{1/4}a_0^{3/4}}\right)}$$

$$\vdots \qquad\qquad\qquad \vdots$$

$$a_{n,f} = (-1)^{\frac{n}{2}-1}\ \frac{\dfrac{2k\alpha b}{\epsilon + k}}{\left(n^2 - 1\right)\pi\left[1 + \dfrac{2s}{3\left(4n^2 - 1\right)} + \dfrac{\epsilon k}{\epsilon + k} + \dfrac{n^2C\tau}{4r^2\sigma^{1/4}a_0^{3/4}} + \dfrac{C\tau}{2p^2\sigma^{1/4}a_0^{3/4}}\right]}$$

$$\text{(n even)}$$

$$a_{3,f} = a_{5,f} = a_{7,f} = \ldots = 0$$

(28)

The subsequent treatment is the same as for the case without heat pipes.

Calculations for a few cases showed that the increase in $T_{max} - T_{min}$ over that for the infinite cylinder was relatively small. Whereas for the calculated cases without heat pipes, $T_{max} - T_{min}$ increased by large factors (up to 15) relative to the values for the infinite cylinder (fig. 7), calculations for the comparable cases with heat pipes showed increases of only about 25 percent. Thus, the isothermalizing effect of conduction to or from the heat pipes remains the dominant factor. Calculations for a similarly insulated and painted 15-cm-radius cylinder without heat pipes showed that also for that case the isothermalizing effect of conduction restricted the increase to only a few percent.

Use of a Heated Isothermal Collar To Provide
Longitudinally Uniform Temperature

Basic equations.- The sketch shows again an open-ended tube, except that near the end, along a section between $x = m$ and $x = n$, the wall is maintained at a slightly elevated uniform temperature by means of heat input from some external source. We suppose, for the present, that the tube axis is normal to the sun's rays and that the insulation is uniform. Along the isothermal section, let $\sigma T^4 = q$; and along the inner and outer sections, where the temperatures, in general, are not constant, let $\sigma T^4 = z(x)$ and $y(x)$, respectively. (See sketch (i).)
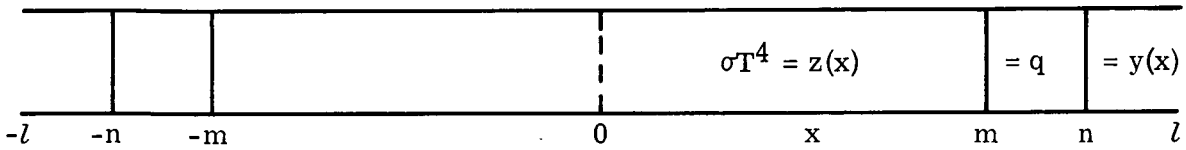
Sketch (i)

The determination of $z(x)$ and $y(x)$ involves the solution of two simultaneous integral equations. The procedure will be only outlined, since it is not very different from what has already been presented. The equation for $z(x)$ is

$$z(x) = c\left[a_0 - z(x)\right] + \frac{1}{2}\int_{-m}^{x} z(\xi)\, e^{\xi-x}d\xi + \frac{1}{2}\int_{x}^{m} z(\xi)\, e^{x-\xi}d\xi + \frac{1}{2}\int_{m}^{n} q e^{x-\xi}d\xi$$

$$+ \frac{1}{2}\int_{-n}^{-m} q e^{\xi-x}d\xi + \frac{1}{2}\int_{n}^{l} y(\xi)\, e^{x-\xi}d\xi + \frac{1}{2}\int_{-l}^{-n} y(\xi)\, e^{\xi-x}d\xi \qquad (29)$$

When this equation is differentiated twice with respect to x, it yields the differential equation

$$\frac{d^2z}{dx^2} = \frac{c}{1+c}(z - a_0)$$

Since z is continuous at $x = 0$ and also must be symmetrical with respect to $x = 0$, it must be of the form

$$z = a_0 + A \cosh fx \qquad\qquad \left(f \equiv \sqrt{\frac{c}{1+c}}\right) \qquad (30)$$

The integral equation for y is

$$y(x) = c\left[a_0 - y(x)\right] + \frac{1}{2}\int_{-l}^{-n} y(\xi)\, e^{\xi-x}d\xi + \frac{1}{2}\int_{n}^{x} y(\xi)\, e^{\xi-x}d\xi + \frac{1}{2}\int_{x}^{l} y(\xi)\, e^{x-\xi}d\xi$$

$$+ \frac{1}{2}\int_{-n}^{-m} q e^{\xi-x}d\xi + \frac{1}{2}\int_{m}^{n} q e^{\xi-x}d\xi + \frac{1}{2}\int_{-m}^{m} z(\xi)\, e^{\xi-x}d\xi \qquad (31)$$

After differentiating twice, it yields

$$\frac{d^2y}{dx^2} = \frac{c}{1+c}\left(y - a_0\right)$$

Although y is symmetrical with respect to $x = 0$, it is not defined over the inner region ($x = -n$ to n); hence, the solution must be assumed in the more general form

$$y = a_0 + B e^{f|x|} + C e^{-f|x|} \qquad (32)$$

In order to solve for A, B, and C, set up three simultaneous equations:

(1) Substitute expressions (30) and (32) for z and y into equation (29) and perform the indicated integrations for $x = 0$.

(2) Similarly, substitute expressions (30) and (32) into equation (31) for y and perform the indicated integrations for $x = n$ and for $x = l$.

The three simultaneous equations in A, B, and C that are thus derived are here set down since this configuration is of special interest:

From $z(0)$,

$$A\left\{\frac{1}{2}\left[\frac{e^{(f-1)m}}{f-1} - \frac{e^{-(f-1)m}}{f+1}\right]\right\} + B\left[\frac{e^{(f-1)l} - e^{(f-1)n}}{f-1}\right] + C\left[\frac{e^{-(f+1)n} - e^{-(f+1)l}}{f+1}\right]$$

$$= a_0\left(e^{-m} + e^{-l} + e^{-n}\right) + q\left(e^{-n} - e^{-m}\right) \qquad (33)$$

From $y(n)$,

$$A\left\{\frac{e^{-n}}{2}\left[\frac{\sinh(1+f)m}{1+f} + \frac{\sinh(1-f)m}{1-f}\right]\right\}$$

$$+ B\left\{\frac{\cosh n}{1-f}\left[e^{(f-1)n} - e^{(f-1)l}\right] - (1+c)e^{fn}\right\}$$

$$+ C\left\{\frac{\cosh n}{1+f}\left[e^{-(1+f)n} - e^{-(1+f)l}\right] - (1+c)e^{-fn}\right\}$$

$$= a_0\left(e^{-n}\sinh n + e^{-l}\cosh n - e^{-n}\sinh m\right) + q e^{-n}(\sinh m - \sinh n) \qquad (34)$$

From $y(l)$,

$$A\left\{\frac{1}{2}\left[\frac{\sinh(1+f)m}{1+f}+\frac{\sinh(1-f)m}{1-f}\right]\right\}$$

$$+B\left[\frac{e^{(f-1)n}-e^{(f-1)l}}{2(1-f)}+\frac{e^{(1+f)l}-e^{(1+f)n}}{2(1+f)}-(1+c)e^{(1+f)l}\right]$$

$$+C\left[\frac{e^{-(1+f)n}-e^{-(1+f)l}}{2(1+f)}+\frac{e^{(1-f)l}-e^{(1-f)n}}{2(1-f)}-(1+c)e^{(1-f)l}\right]$$

$$=a_0(\cosh l-\sinh m+\sinh n)+q(\sinh m-\sinh n) \tag{35}$$

For a given geometry and set of parameters (m, n, l, a_0, c (hence f), and q), one can evaluate the coefficients of A, B, and C in these three equations and then solve simultaneously for the numerical values of A, B, and C.

Uniform-temperature inner section.- A more interesting problem is to set $A = 0$ and solve for B, C, and q from equations (33), (34), and (35); that is, determine the temperature (since $q = \sigma T^4$) of the heated collar that will provide a uniform temperature between $x = 0$ and $x = m$. (The uniformity corresponds to having set $A = 0$.) For this case, since equation (30) simply reduces to $z = a_0$ $(0 < x < m)$, the uniform temperature is the same as would exist in a similarly painted infinite cylinder. With B, C, and q thus known, calculation of the heat that must be put into the collar in order to keep it at the required temperature is straightforward. At any longitudinal location on the heated collar, the required heat input per unit area is the heat transmission outward through the insulation $c(q - a_0)$ plus the heat radiated inward q minus the heat received by radiation from the inside of the cylinder. This last item must be determined as the sum of exponential type integrals along the five sections of the cylinder ($-l$ to $-n$, $-n$ to $-m$, $-m$ to m, m to n, n to l, where the integral from m to n must be in two parts — m to x and x to n). The derived expression for the required rate of heat input per unit area must finally be integrated over the collar.

Calculated results.- A number of calculations were made of the temperature distributions and of the corresponding heating powers for a tube of length $l = 12$ radii with a uniform-temperature collar between $x = 6$ and $x = 8$ (that is, $m = 6$ and $n = 8$). The results are shown in figure 8. (Fig. 8(a) is for $\alpha = 0.25$, $\epsilon = 0.85$, $k = 0.0025$; and fig. 8(b) is for $\alpha = 0.15$, $\epsilon = 0.85$, $k = 0.0025$.) The most significant numerical results are given in the tables in the figures. (The results for total heat power input to the collar are for a tube radius of 150 cm.)

The difference between the wall temperatures at $x = 0$ and at $x = 6$ may be taken as a measure of the temperature uniformity in the 6-radius-long section between the mirror and the collar. For the "design conditions" (the bottom lines of both tables), the temperatures at $x = 0$ and at $x = 6$ are equal and about $2°$ below the collar temperature. In the worst case (the third line of the table in fig. 8(a)), the telescope was assumed to be completely in shadow, or alined with the sunlight, so that there was no external radiation input. For this case, the temperature at $x = 6$ is $2.4°$ higher than that at $x = 0$, and is $3.6°$ cooler than the collar.

The 300- to 400-watt input required to maintain the collar at the specified temperature seems relatively modest; and extending the length of the shield (the section from n to l) would reduce it to lower values. Furthermore, relatively small amounts of additional power applied in the section between the mirror and the collar could maintain a uniform and constant temperature along that section regardless of the tube orientation relative to the sunlight.

The heat source for the collar is a rather challenging design problem. One might use some arrangement with variable-conductance heat pipes leading from an isotope power unit or from solar-heating panels provided with some phase-change material to furnish heat during the shadow phase of the orbit. In any case, some small additional electric power would seem to be necessary if very fine control of the temperature is needed.

Tube With Nonuniform Insulation and Paint

In all the preceding analyses and examples, the thermal-control coating and insulation blanket, as characterized by α, ϵ, and k, were assumed to be perfectly uniform along the tube. Actually, as previously indicated, the thermal conductance of a super-insulation blanket is sensitive to relatively minor irregularities in construction or application – for example, the closeness with which the layers are packed. Also, different batches of paint might show some variations, especially in the rate of darkening during exposure to the ultraviolet and particle radiation in space. Some calculations were therefore made to determine the effect of changing the values of α and k over a given length of an infinite cylinder normal to the solar rays. The simplified geometry was considered to be adequate for demonstrating how the effect of an irregularity is washed out along a finite cylinder.

The geometry and definitions are indicated in sketch (j). The subscript 1 is used to indicate properties along the variant section between $x = -l$ and $x = l$; the subscript 0 is used to indicate the properties of the remainder of the cylinder that extends to infinity in both directions.

Sketch (j)
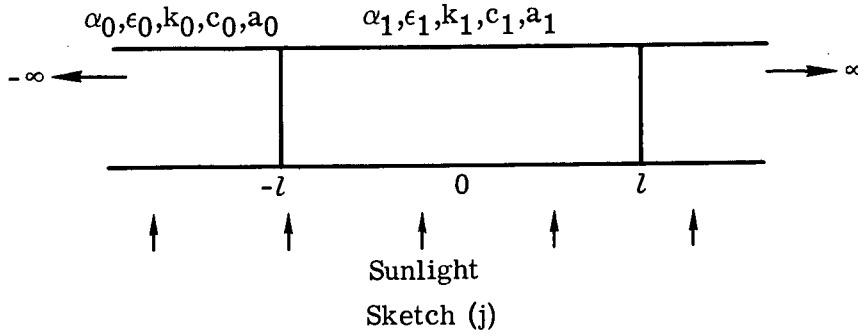
The mathematical analysis will not be given, since it is similar to the analyses of the preceding problems. The solutions are of the form

$$z_1 = a_1 + A \cosh f_1 x \qquad (|x| < l)$$

$$z_0 = a_0 + B e^{-f_0 |x|} \qquad (|x| > l)$$

where

$$a_0 = \frac{\alpha_0 b}{\pi \epsilon_0}, \qquad a_1 = \frac{\alpha_1 b}{\pi \epsilon_1}$$

$$f_0 = \sqrt{\frac{c_0}{1 + c_0}}, \qquad f_1 = \sqrt{\frac{c_1}{1 + c_1}}$$

As before, A and B are determined by solving two simultaneous equations, as for $z_1(0)$ and $z_0(l)$.

Figure 9 shows some of the calculated temperature distributions. For all cases, α_0 was taken as 0.15 and α_1 was taken as 0.25. The difference is considerably more than should exist in an actual case. The value of ϵ was assumed to be 0.85 for all cases, since ϵ does not change appreciably from one batch of paint to another and is not much affected by radiation. In some cases, the value of k_1 was taken as twice the value of k_0; in others, k_1 and k_0 were equal. A considerable range of l values was used.

For the uninsulated conditions, the curves show large discontinuities, the temperatures rapidly approaching those for the infinite cylinders at short distances from the discontinuities. For all cases in which there was any insulation at all, the effect of the changed α or k is distributed over a considerable length of the cylinder. There is a small discontinuity (0.1° to 1°) at the edge of the variant section, which would be somewhat smoothed out in a practical case, not only because of wall conduction but also because changes in insulation characteristics would probably be fairly gradual rather than discontinuous. Admittedly, the α and k variations used in these examples are

33

not very realistic. The α variation is probably unreasonably large; and the k variation, although not exaggerated, would probably be randomly distributed. Nevertheless, it seems clear that one cannot hope to predict temperatures and temperature distributions very precisely for a range of conditions simply on the basis of nominal paint and insulation characteristics or on the basis of model tests. Precision temperature control will hardly be achieved without some active controls such as are referred to in the preceding section.

On Maintaining Uniform and Constant Temperature

Thermal distortions might occur if the telescope temperatures are allowed to change, not only because different parts of the telescope may have different thermal-expansion coefficients but also because the different parts would change their temperatures at different rates. It seems advisable, therefore, to strive not only for uniformity but also for constancy of temperature.

It was previously shown that a heated collar near the open end of the telescope tube can, under ideal conditions, provide a uniform temperature along the main part of the tube (between the mirror and the collar). The uniform temperature in this case is that which would be acquired by a similarly painted and insulated infinite cylinder at the same orientation relative to the incident radiation. If the orientation of the tube relative to the radiation is changed, a different collar temperature could then provide the same mean temperature along the tube; however, the temperature will no longer be uniform along the tube, although the nonuniformity may not be very large. Thus, a heated collar alone cannot suffice to maintain the tube temperature both uniform and constant as the orientation (hence the radiation input) is varied.

One approach to uniformity and constancy might be to use the highest temperature condition (the tube axis normal to the solar rays) to define the design temperature, and add additional heat along the tube to maintain this uniform temperature for all other orientations. For k = 0.0025, this additional heating for the 150-cm-radius tube would be only about 50 watts for the worst case (no external radiation input at all, as with the tube axis parallel to the solar rays).

Longitudinal heat pipes.- A method of maintaining a more uniform temperature along the tube would be to provide a set of longitudinal heat pipes. If, in addition, these longitudinal heat pipes were thermally connected together, they would also contribute to improving the circumferential temperature uniformity. In reference 4 it was suggested that a shallow drumlike vapor chamber might be located just under the mirror, and that the longitudinal heat pipes might be brought into the vapor chamber, as indicated in sketch (k). Such an arrangement would provide not only a uniform radiation environment for the bottom of the mirror, but would also insure that the temperature of this radia-

34
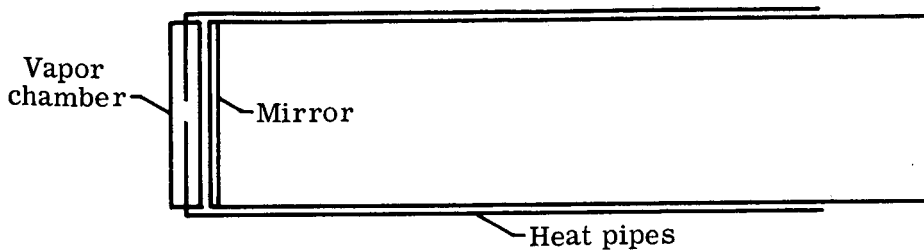
Sketch (k)

tion was very nearly the same as that of the telescope tube itself. However, actual construction of a flightworthy vapor chamber of this type and size with many inserted heat pipes seems a rather formidable undertaking. Perhaps merely bonding the heat pipes to the outer top or bottom surface of the vapor chamber would be adequate.

Balloon-type enclosures.- In reference 1 it was suggested that the thermal problem could be eased by enclosing the entire telescope in a balloon. The thermal-radiation environment within such a balloon should be nearly uniform and isotropic and should also be nearly independent of orientation relative to the external radiation, provided the inner surface of the balloon is nearly specular. Reference 17 contains some space-simulation-chamber studies of the radiation inside a model balloon irradiated by a solar simulator. On the whole, the data tend to confirm the prediction. For example, in one case, the external surface had a mean α/ϵ ratio of 1.15 (for which the mean internal temperature was 290 K), the internal surface was lightly anodized, and the outer surface of the "telescope tube" was specular. The temperature of the radiation striking the outside surface of the telescope tube (sketch (l)) was found to be uniform to within about ±5 K for a range of orientations. This uniformity, considered in terms of (radiation temperature)[4], is over 20 times better than for

Sketch (l)

an unenclosed tube irradiated from one side by sunlight. Furthermore, the mean temperature of the radiation incident on the tube was, as expected, almost independent of the orientation of the tube relative to the solar-simulator beam.
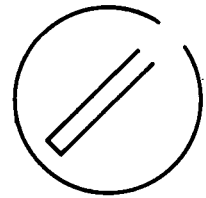
Thus, the balloon could be very helpful in providing relatively constant and circumferentially uniform temperatures. Furthermore, if the balloon were extra large, with a diameter considerably exceeding the telescope length (sketch (m)), the longitudinal non-uniformity, with decreasing temperatures toward the open end (as shown in fig. 6), could also be greatly reduced. (Such a spacious volume around the telescope was probably intended in ref. 1; in fact, it mentioned a set of concentric balloons.) More extreme uniformity and constancy would require additional complexity, such as the previously discussed vapor chambers, heat pipes, heated collars,
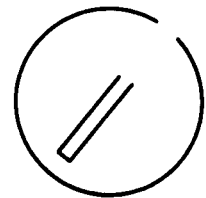
Sketch (m)

fine-control heating power, and insulation; however, the performance requirements of all such components would now be greatly reduced.

Thus, a well-insulated telescope enclosed within an extra-large balloon and provided with perhaps 150 watts (for the 150-cm-radius telescope) of distributed and regulatable heating power appears to be an attractive concept. Certain inherent elements of awkwardness in the concept have probably prevented its serious consideration in such systems studies as that of reference 18. For example, the balloon could not be a simple sheet, like the Echo satellites, but would have to be sufficiently stiff, probably with internal bracing, so that it could be readily reoriented as required. The large solar-cell panels extended from the side of the telescope tube in the design proposed in reference 18 would have to be located outside of the sphere, somehow attached to the bracing. A torn area, such as might be produced during deployment, might not seriously affect the thermal control, but might let in sunlight that would be reflected around the inside of the balloon and into the telescope. During the shadow phase, the temperature inside the balloon would drop, so that consideration would still have to be given to means of preventing periodic variations of telescope temperature in response to the alternating sunlight and shadow of a low orbit.

LOCAL WALL HEATING VARIATION DURING ORBIT

If the telescope is in a fairly close orbit about the earth, it will experience alternating phases of sunlight and shadow, with a period of about 100 minutes; or, if it is in a geosynchronous orbit, it may experience daily shadow periods lasting as long as 1 hour. The question now arises as to whether a fairly well insulated telescope would experience any significant heat-input oscillations in response to the unsteadiness of the thermal input to the outer skin.

Any analysis of this problem for a relatively undefined structure, and without a thorough knowledge of the characteristics of unsteady heat flow through multilayer insulation would seem to carry a rather heavy burden of assumptions. Some experiments in a space-simulation chamber will be needed in order to procure the basic quantitative data. For present purposes it was considered that a simplified analysis would suffice to provide some insight into the problem.

Consider that the insulation consists of 50 aluminized plastic sheets, each 0.00075 cm thick. A "radiation conductance" of 0.0025 was assumed, as in many of the calculated examples. However, this value corresponds theoretically to only about 10 sheets, since the radiation conductance between a pair of adjacent sheets is about half the emissivity of the aluminized plastic sheet, or 0.025. Accordingly, the 50 sheets were represented, for the analysis, by 10 sheets, each five times as thick as an actual single

sheet, or 0.00375 cm thick; and the radiation conductance between adjacent pairs of sheets was retained as 0.025.

The temperatures of the 10 sheets, starting with the outside sheet, are designated T_0, T_1, . . ., T_9; and the temperature of the cylinder wall is designated T_{10}. The wall temperature T_{10} is assumed to be controlled to a constant value, equal to that for an infinite tube with the given α and ϵ oriented normal to sunlight. The outside sheet quickly attains radiation equilibrium with the environment, so that its temperature is assumed to be known as a function of time. One may then set up nine equations for the other temperatures T_1, T_2, . . ., T_9:

$$\left.\begin{array}{l} 0.025\sigma\left(T_0{}^4 + T_2{}^4 - 2T_1{}^4\right) = 0.00375 \times 0.4 \, \dfrac{dT_1}{dt} \\[3em] 0.025\sigma\left(T_1{}^4 + T_3{}^4 - 2T_2{}^4\right) = 0.00375 \times 0.4 \, \dfrac{dT_2}{dt} \\[2em] \qquad\qquad \vdots \qquad\qquad\qquad\qquad \vdots \\[2em] 0.025\sigma\left(T_8{}^4 + T_{10}{}^4 - 2T_9{}^4\right) = 0.00375 \times 0.4 \, \dfrac{dT_9}{dt} \end{array}\right\} \qquad (34)$$

where the plastic is assumed to have unit density and a specific heat of 0.4.

Calculations were made for four cases. For each case, the nine temperatures T_1, T_2, . . ., T_9 were determined as functions of time. However, only T_9 (the temperature of the sheet immediately adjacent to the wall) will be shown, since it determines directly the rate of radiation heat input to the wall from the outside. The calculations were made only for a subsolar area.

Synchronous Orbit

For a synchronous orbit, the subsolar area was assumed to have an outside temperature T_0 that is constant at 396 K except for 1 hour when it is essentially zero. The wall temperature T_{10} was assumed to be constant at 297.4 K (corresponding to $\alpha = 0.25$, $\epsilon = 0.85$). Figure 10 shows the response of T_9 to the 1-hour shadow phase. Two curves are shown. The curve with the deeper dip is for 50 layers of aluminized plastic; the other is for 100 layers. The analysis for the latter case merely required that the factor 0.00375 in equations (34) be changed to 0.0075 (since each of the 10 sheets is now considered to be ten times as thick as an actual single sheet).

The lag and the spreading out of the response are very apparent. For the thinner insulation, there is essentially no response for the first 15 minutes after the beginning of the shadow phase, the minimum is reached about 1/2 hour after the end of the shadow

phase, and the entire perturbation lasts about 4 hours. For the thicker insulation, the initial lag is about 30 minutes, the minimum is less deep and occurs about 1 hour after the end of the shadow phase, and the entire perturbation lasts about 7 hours.

Spreading the response over several hours is a useful function of the heavy multi-layered insulation. The solar heat input to the wall of the entire telescope tube may be, say 40 watts; so during the 1-hour shadow phase, a 40-watt-hour deficit occurs, which must be supplied from other sources — probably electrical — if the wall temperature is to remain constant. The fact that the response is spread over, say, 7 hours means that an average power of only 6 watts is needed during this period. For exact compensation, however, about 20 watts would be needed for the period when T_9 is near its minimum (or 32 watts for the thinner insulation).

The time between emergence from shadow and return of T_9 to its normal value (about 3 hours for the 50-layer blanket and about 6 hours for the 100-layer blanket) may be taken as a rough indication of the time required after a reorientation of the telescope for T_9 to attain its new equilibrium value.

Low Orbit

For the low orbit, alternating sunlight and shadow phases of 60- and 40-minute durations, respectively, were assumed. The wall temperature T_{10} was again taken as 297.4 K, and, for the subsolar area under consideration, the temperature of the outermost layer T_0 was assumed to be 396 K when in sunlight and 244 K when in shadow. This variation, shown in the upper curve of figure 11, is obviously a gross simplification of any actual case, but it should be adequate for present purposes. The calculations were made, as for the preceding problem, for 50-layer and 100-layer insulation blankets.

The lower curves of figure 11 show the calculated variation of T_9 with time. The oscillation of T_9 lags that of T_0 by about 45 minutes for the 50-layer blanket, and by about 75 minutes for the 100-layer blanket. The amplitude of the oscillation is four times as much for the 50-layer blanket as for the 100-layer blanket. Thus, the heavier blanket provides a strong damping of the oscillating input, but the oscillation of T_9 for the lighter blanket is a fairly large fraction of the mean difference between T_9 and the wall temperature T_{10}. Furthermore, since the amplitude seems to vary inversely as the square of the number of layers, it would probably increase rapidly with further decrease in the number of layers.

RÉSUMÉ AND CONCLUDING REMARKS

Analytical methods have been developed for estimating the temperature distribution in a large space telescope, idealized as a simple insulated cylindrical tube, open at one

end, and with a flat perfect mirror across the other end. Since heat transfer, both within the tube and through the insulation, is mainly by radiation, σT^4 was taken as the basic variable (where σ is the Stefan-Boltzmann constant and T is the temperature). Expressing the circumferential distribution of σT^4 as a Fourier series permitted a straightforward determination of the circumferential distribution; and use of an exponential expression to approximate the view factor between circular bands of the tube provided tractable equations for the longitudinal temperature distribution. Methods for taking into account the effects of multilayer insulation, thermal-coating characteristics, heat pipes, and heated collars were also developed.

A few numerical calculations were made to show the significance of each of these components. The cylinder radius was taken as 150 cm for most of the calculations. Where wall conduction was involved, the wall was assumed to be of 0.1-cm-thick aluminum. Where circumferential heat pipes were considered, they were assumed to be 40 cm apart. The cylinder axis was taken as normal to the solar rays, and the shadowed half was assumed to receive no radiation input at all. These assumptions can be altered without significant modification of the analytical methods.

If the tube is wrapped in a multilayer insulation, the circumferential temperature nonuniformity can be limited to tenths of a degree. If, in addition, circumferential heat pipes are attached, the nonuniformity can be further reduced to values of the order of hundredths of a degree. A multilayer insulation also tends to minimize any temperature irregularities of the tube wall due to nonuniformity of the thermal-paint characteristics or of the insulation itself. It can also damp out time variations due to alternating sunlight and shadow of a low orbit. On the other hand, thermal equilibrium, at which the heat transmitted in through the insulation equals the heat radiated out of the open end of the tube, may exist at undesirably low internal temperatures when such insulation is used; also, there will be a large temperature drop along the tube from the mirror to the open end. A heated constant-temperature collar near the open end of the cylinder will largely eliminate both of these problems.

Although this paper is largely concerned with temperature uniformity of the telescope, just how much uniformity is essential or desirable remains an open question. The development of glasses (and perhaps also structural materials) with very low thermal-expansion coefficients, and the development of means for adjusting the mirror figure (known as "active optics") would seem to ease the thermal-control requirements. The availability of these materials and techniques, however, would hardly justify designing for minimal thermal control. For example, even if active optics is used, it would nevertheless be preferable if checking and adjusting the optics were required only occasionally, rather than every few minutes. Other types of technical developments might also appreciably influence the requirements. For example, the main structure between the primary

and secondary mirrors might be a tubular framework, constructed as one continuous heat pipe.

In any case, the purpose of the present paper is not to propose or advocate any particular degree of temperature control or any particular means of attaining it, but rather to present some practical analytical methods and some calculated results for a first-approximation configuration.

Langley Research Center,
National Aeronautics and Space Administration,
Hampton, Va., January 16, 1973.

REFERENCES

1. Spitzer, Lyman, Jr.: The Beginnings and Future of Space Astronomy. Amer. Sci., vol. 50, Sept. 1962, pp. 473-484.

2. Anon.: Optical Telescope Technology. NASA SP-233, 1969.

3. Robertson, Hugh J.: Development of an Active Optics Concept Using a Thin Deformable Mirror. NASA CR-1593, 1970.

4. Katzoff, S.: Considerations on Precision Temperature Control of a Large Orbiting Telescope. Optical Telescope Technology, NASA SP-233, 1969, pp. 417-424.

5. Hrycak, Peter, and Helgans, R. E., Jr.: Equilibrium Temperature of Long Thin-Walled Cylinders in Space. Chem. Eng. Progr. Symp. Ser., vol. 61, no. 59, 1965, pp. 172-178.

6. Jakob, Max: Heat Transfer. Vol. II. John Wiley & Sons, Inc., c.1957.

7. Graham, John D.: Radiation Heat Transfer Around the Interior of a Long Cylinder. J. Spacecraft, vol. 7, no. 3, Mar. 1970, pp. 372-374.

8. Sparrow, E. M.: Radiant Absorption Characteristics of Concave Cylindrical Surfaces. Trans. ASME, Ser. C: J. Heat Transfer, vol. 84, no. 4, Nov. 1962, pp. 283-293.

9. Anon.: Subcritical Life Support Cryogen Storage Using High Performance Insulation. LMSC/HREC D149499, Lockheed Missiles and Space Company, Feb. 1970.

10. Hyde, E. H.: Multilayer Insulation Thermal Protection Systems Technology. Res. Achievements Rev., Vol. IV, rep. no. 2, NASA TM X-64561, 1971, pp. 5-52.

11. Abbott, G. L.: Total Normal and Total Hemispherical Emittance of Polished Metals. Measurement of Thermal Radiation Properties of Solids, Joseph C. Richmond, ed., NASA SP-31, 1963, pp. 293-306.

12. Buckley, H.: On the Radiation From the Inside of a Circular Cylinder. Phil. Mag., Ser. 7, vol. 4, no. 23, Oct. 1927, pp. 753-762.

13. Buckley, H.: On the Radiation From the Inside of a Circular Cylinder – Part II. Phil. Mag., Ser. 7, vol. 6, no. 36, Sept. 1928, pp. 447-457.

14. Buckley, H.: On the Radiation From the Inside of a Circular Cylinder – Part III. Phil. Mag., Ser. 7, vol. 17, no. 7, 1934, pp. 576-581.

15. Yamauti, M. Z.: Recherche d'un Radiateur Intégral au Moyen d'un Corps Cylindrique. P. V. Com. Int. Poids Més., Ser. 2, vol. 15-16, 1933, pp. 243-253.

16. Usiskin, C. M.; and Siegel, R.: Thermal Radiation From a Cylindrical Enclosure With Specified Wall Heat Flux. Trans. ASME, Ser. C: J. Heat Transfer, vol. 82, no. 4, Nov. 1960, pp. 369-374.

17. Sweet, George E.: An Experimental Investigation of Three Balloon-Type Enclosures for Thermal Control of Satellites. NASA TN D-6224, 1971.

18. Anon.: A System Study of a Manned Orbital Telescope. D2-84042-1 (Contract NAS 1-3968), Boeing Co., Oct. 1965. (Available as NASA CR-66047.)
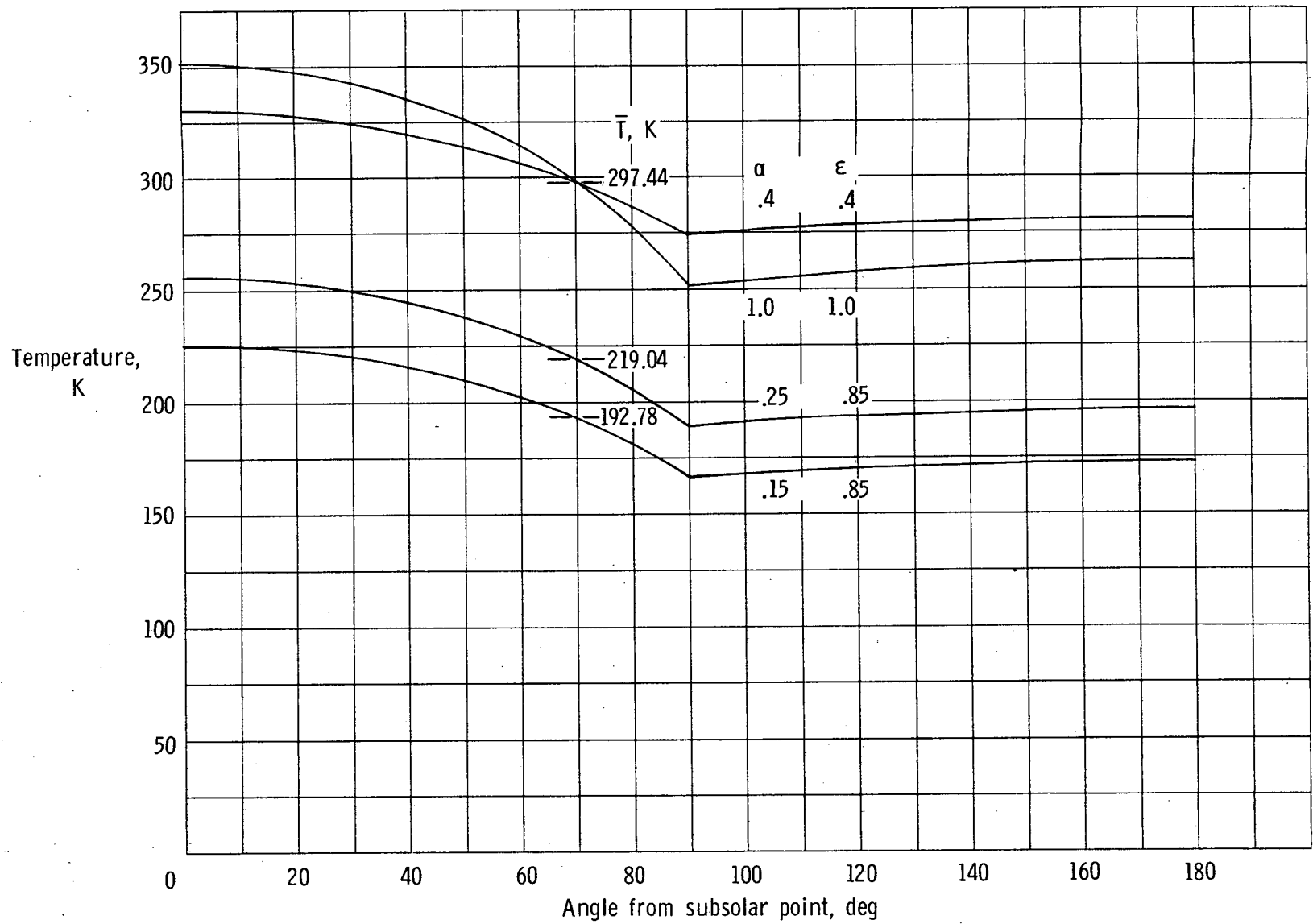
Figure 1.- Temperature distribution around uninsulated infinite cylinder with axis normal to solar rays. No heat conduction along wall.
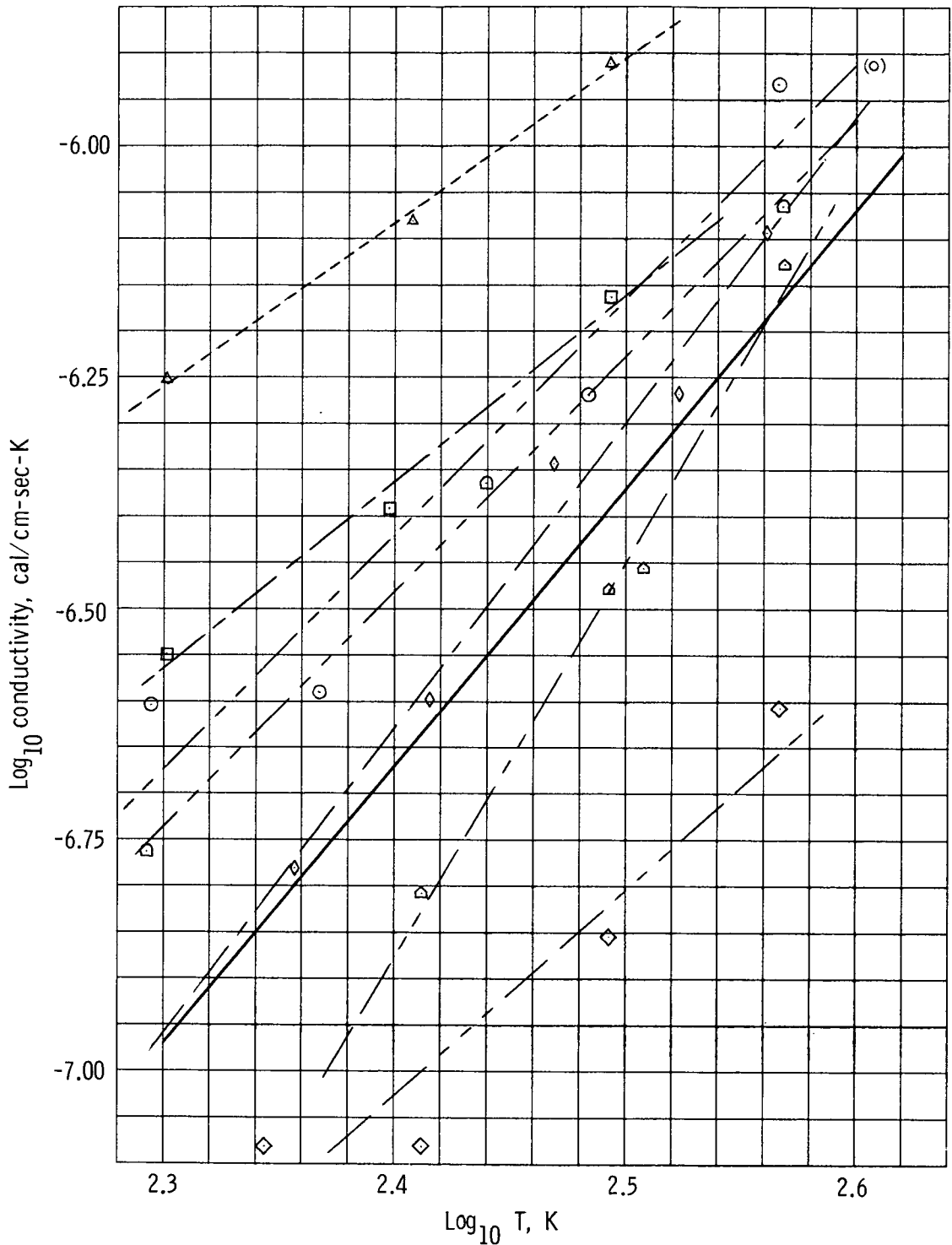
Figure 2.- Measured conductivities of several multilayer insulations, from references 9 and 10. Best-fit straight lines are shown for every set of data. The heavy solid line has a slope of 3 and corresponds to a "radiation conductance" k of 0.0025 for a 1-cm-thick layer (conductivity, $4\sigma T^3 k$). See line key on page 45.

KEY FOR FIGURE 2

Symbol	Construction (layers and separators)	Packing density (layers/cm)
△ – – – – – –	Alternate layers of dimpled singly aluminized Mylar and embossed singly aluminized Mylar	75.5
□ – –	Doubly aluminized Mylar (perforated) – red foam	9.1
○ – – –	Doubly aluminized Mylar – red foam	9.1
○ – – – –	Embossed singly aluminized Mylar – nylon net	19.7
◇ – – –	Doubly aluminized Mylar – fiber-glass tufts	8.7
△ – – – –	Crinkled singly aluminized Mylar (NRC-2)	27.6
◇ – – – – –	Embossed singly aluminized Mylar	63.8

α	ε	$\bar{T}$, K	r, cm
0.25	0.85	219.04	∞ (no conduction)
.25	.85	219.04	150
.40	.40	297.44	150
.15	.85	192.78	150
.40	.40	297.44	15

(a) No insulation.

Angle from subsolar point, deg

$T - \bar{T}$, K
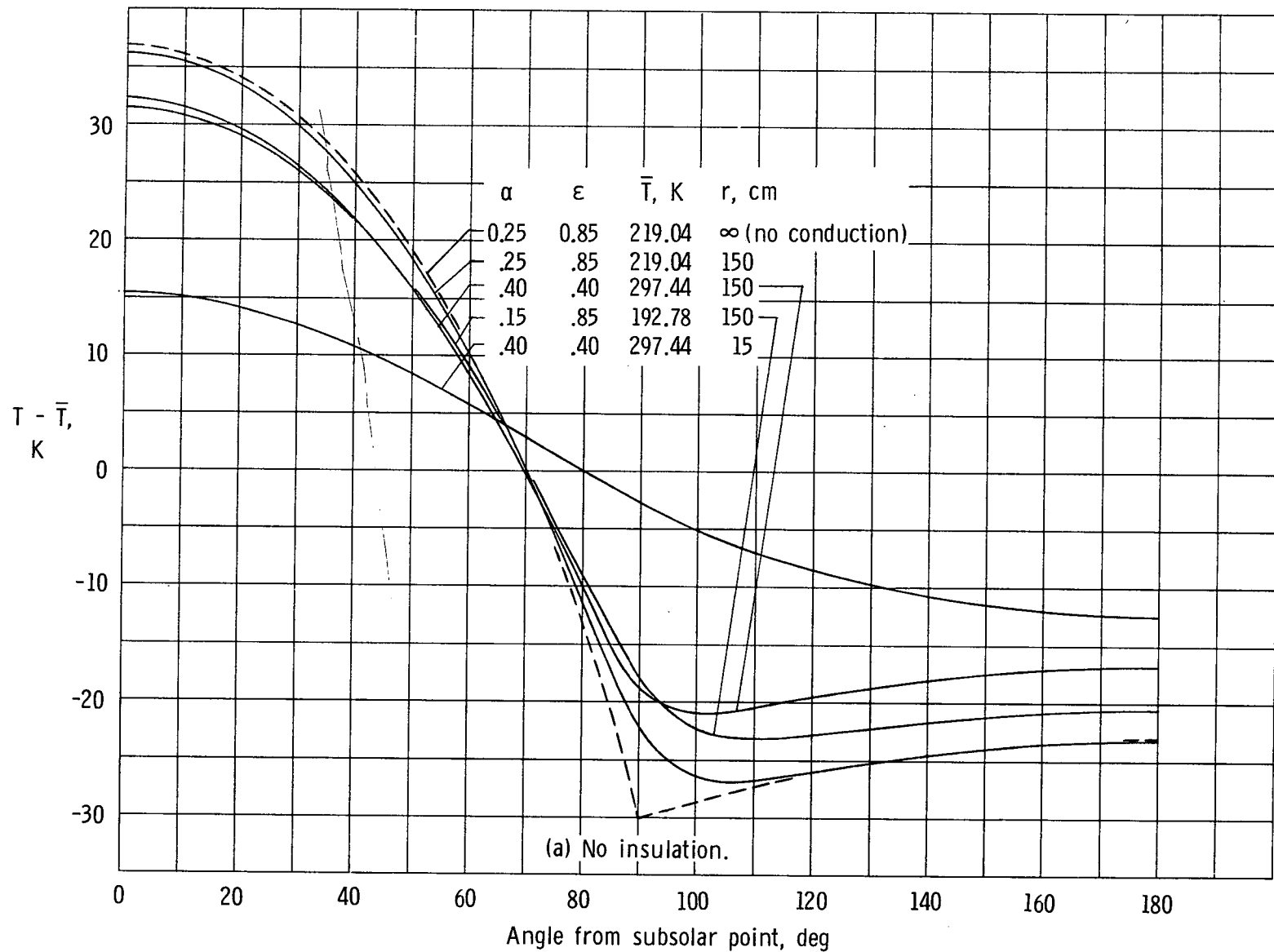
Figure 3.- Temperature distribution around infinite cylinder with axis normal to solar rays. Wall conduction taken into account. Cylinder wall, 0.1-cm-thick aluminum; radius, r = 150 cm unless otherwise noted.
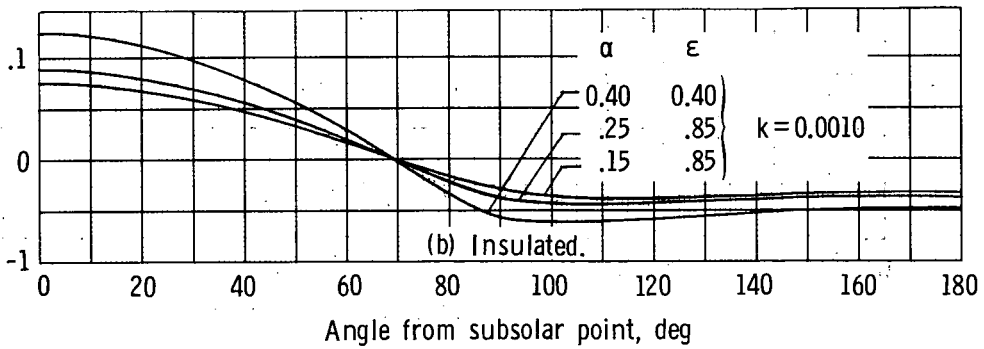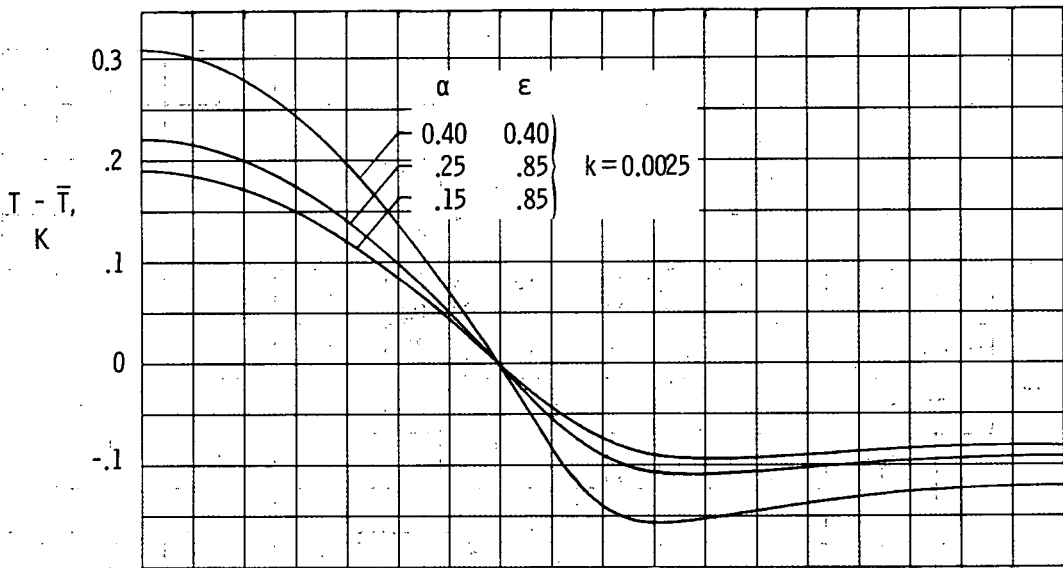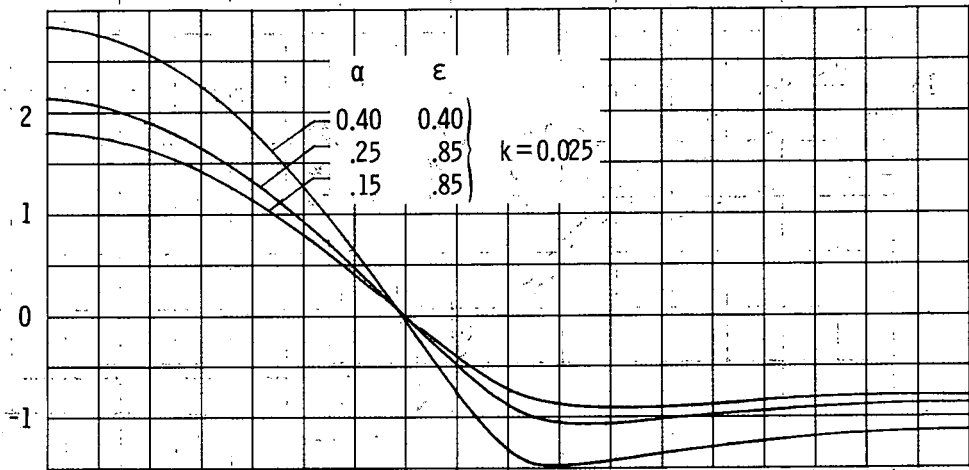
Figure 3.- Concluded.
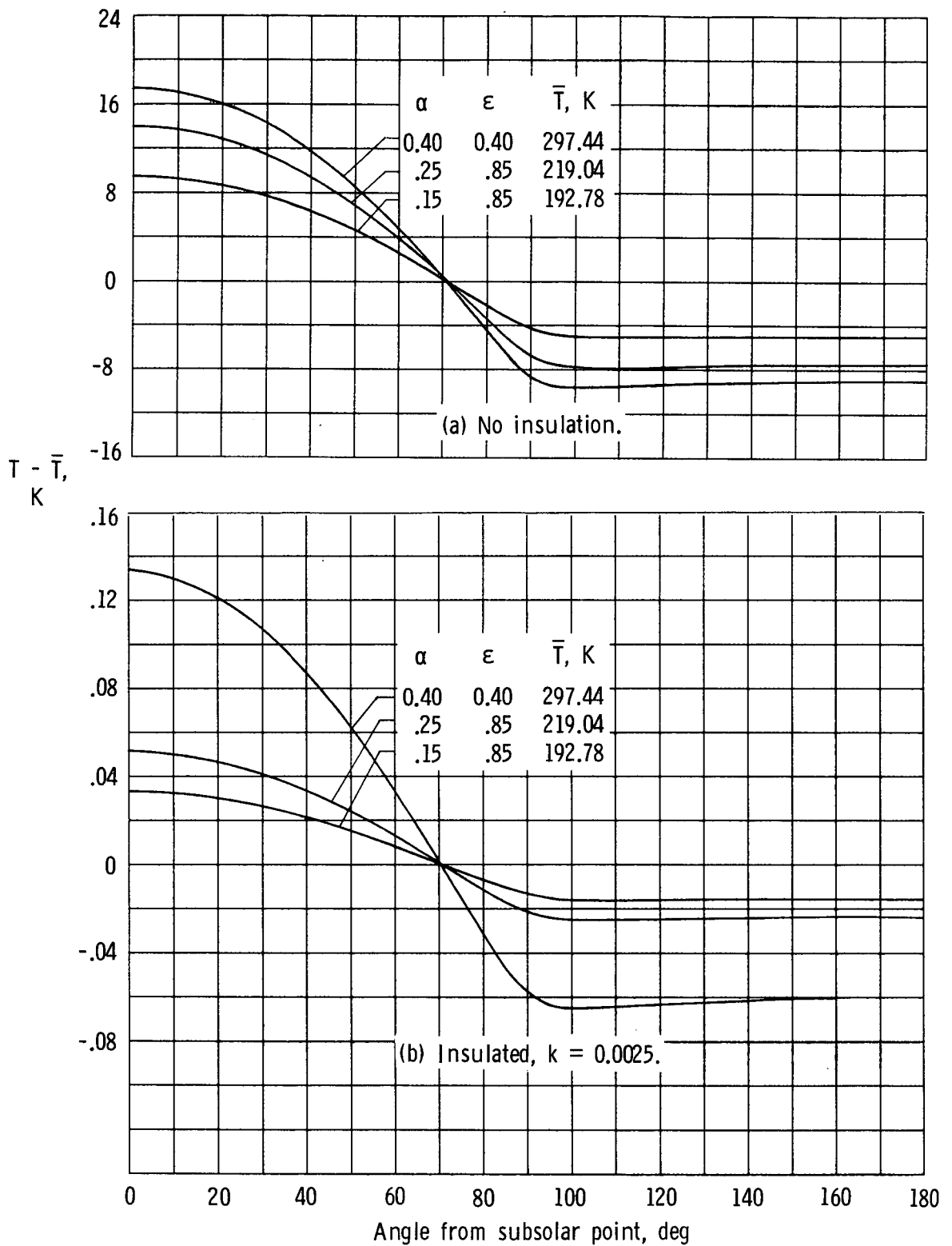
Figure 4.- Temperatures around infinite cylinder with heat pipes at 40 cm. Axis normal to solar rays; radius, 150 cm; wall, 0.1-cm-thick aluminum. Temperatures are on the circle midway between adjacent heat pipes.
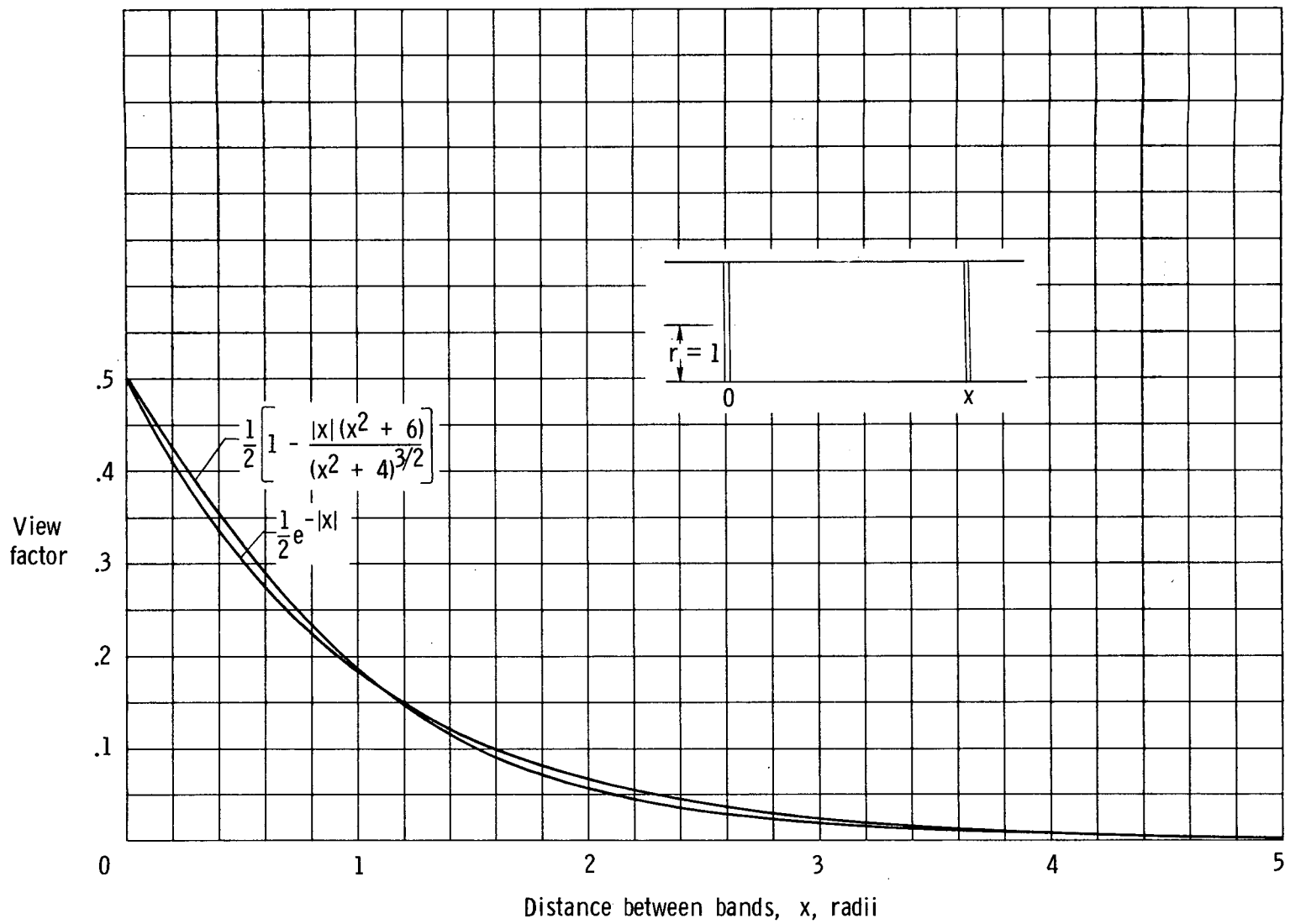
Figure 5.- Comparison of exact with approximate view factor between two circular bands inside a cylinder.
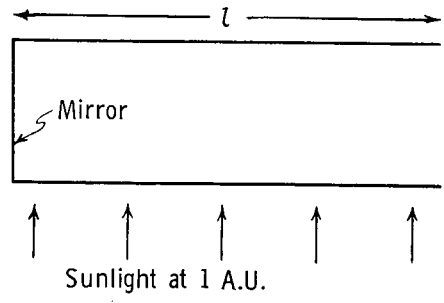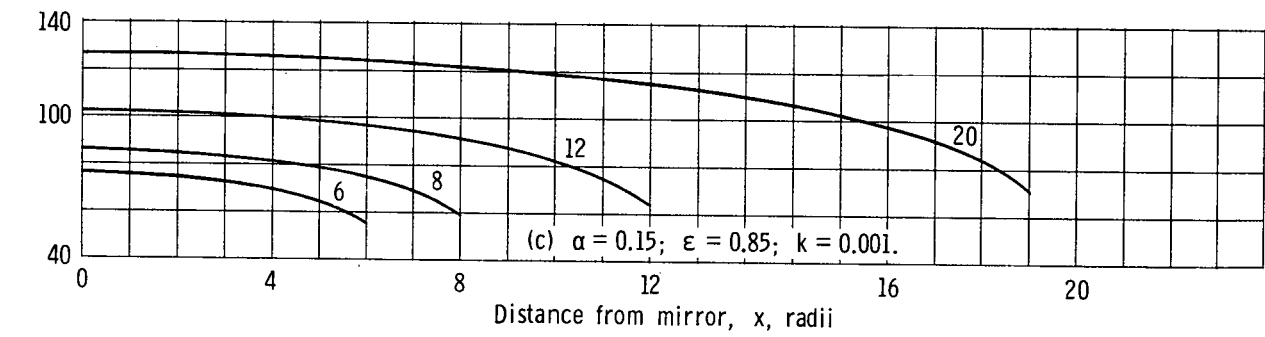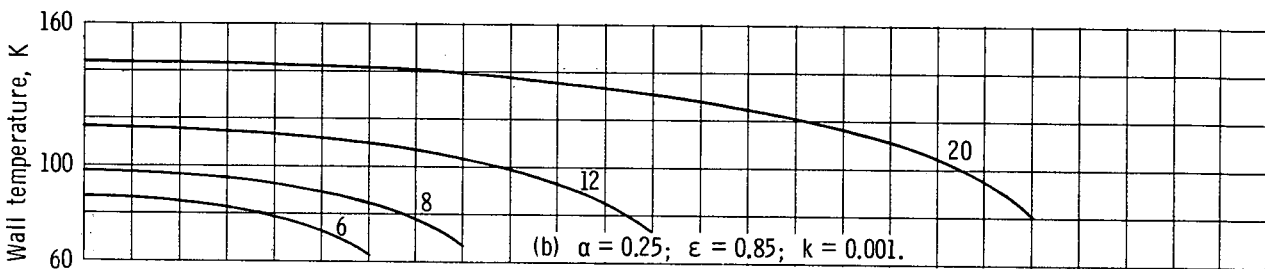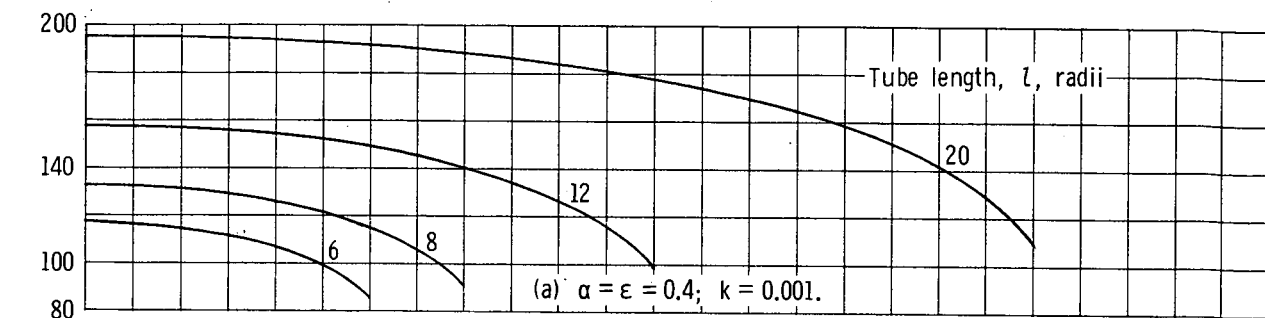
Figure 6.- Variation of temperature (circumferential average) along inside wall of insulated and uninsulated open-ended tubes. Tube axis normal to solar rays.
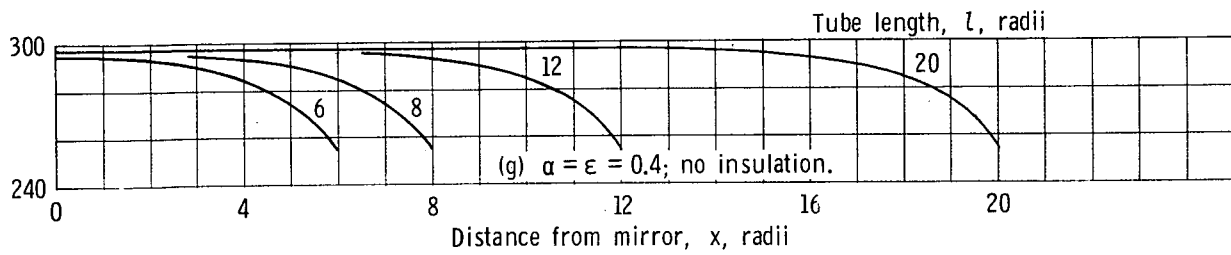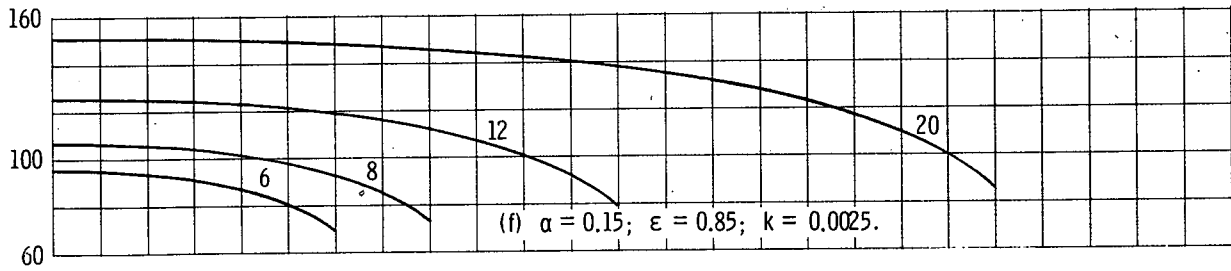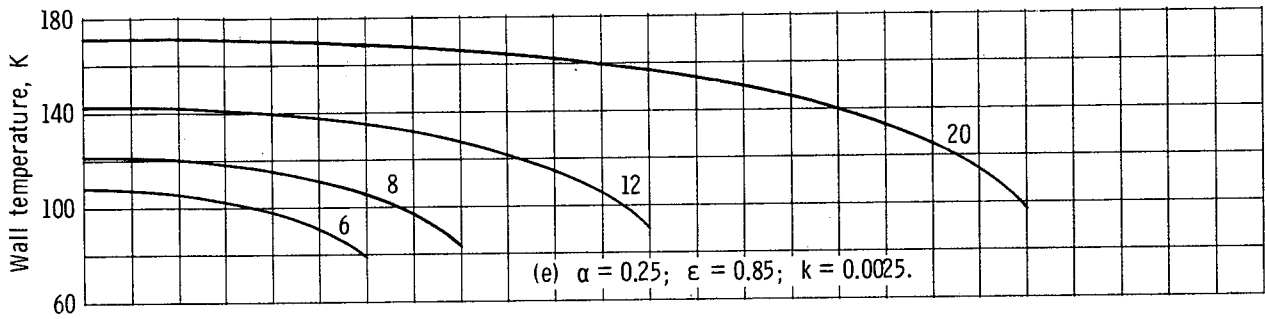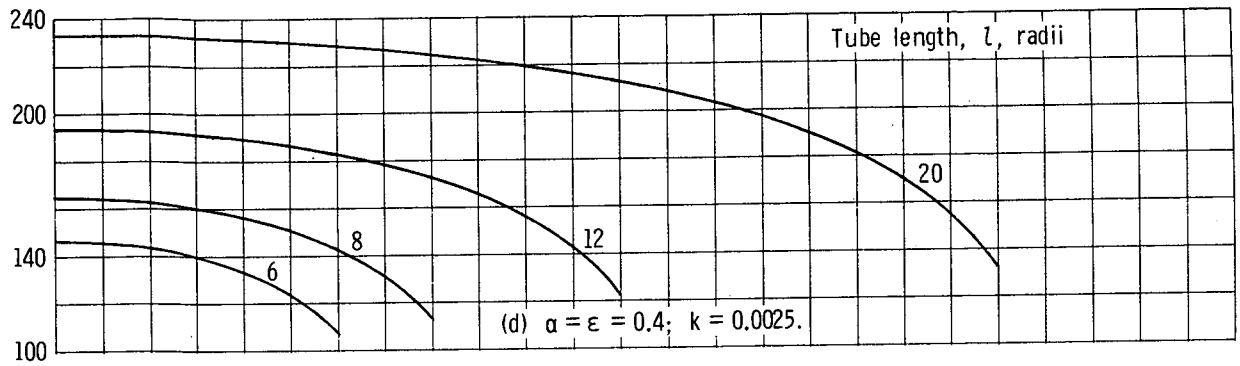
Figure 6.- Continued.

51
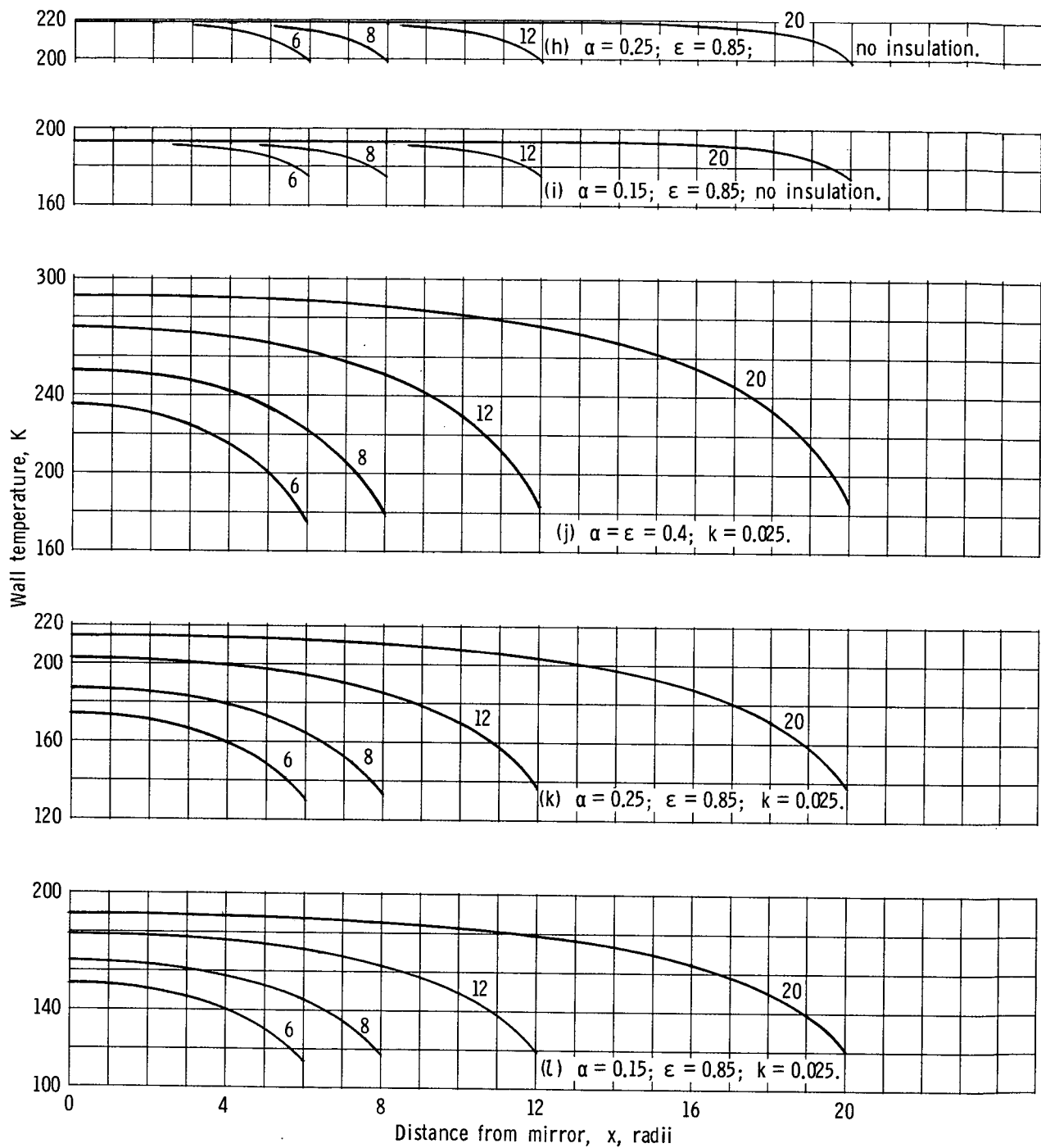
Figure 6.- Concluded.
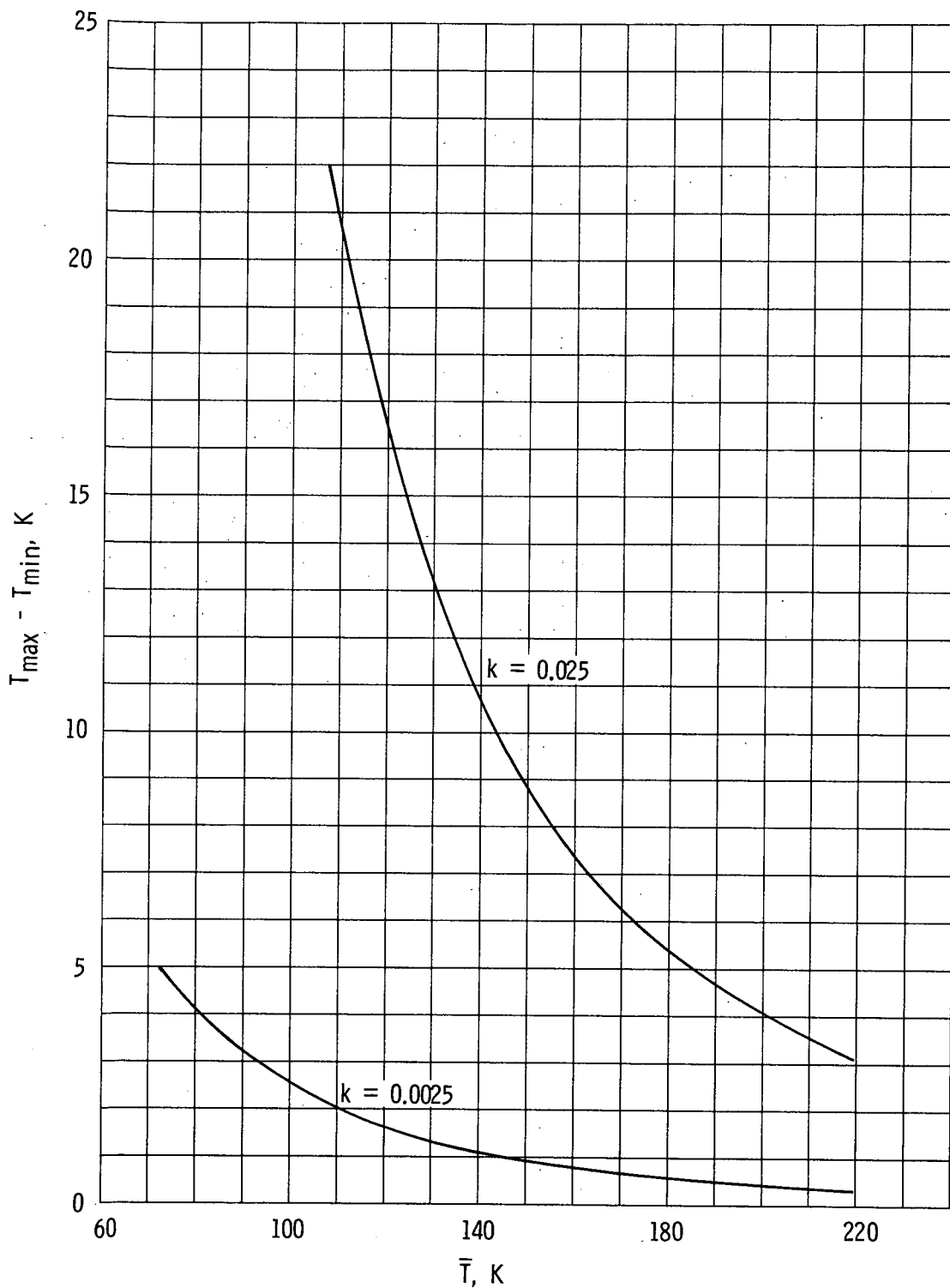
Figure 7.- Difference between maximum and minimum wall temperatures around the cylinder as a function of local root-mean-fourth-power temperature $\overline{T}$ $\left(=(a_0/\sigma)^{1/4}\right)$. Finite-length tube with axis normal to solar rays; $\alpha = 0.25$; $\epsilon = 0.85$; $k = 0.025$ and 0.0025; $r = 150$ cm; no heat pipes.
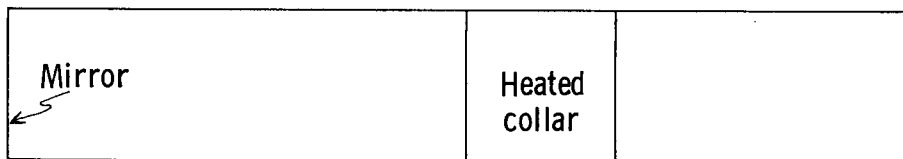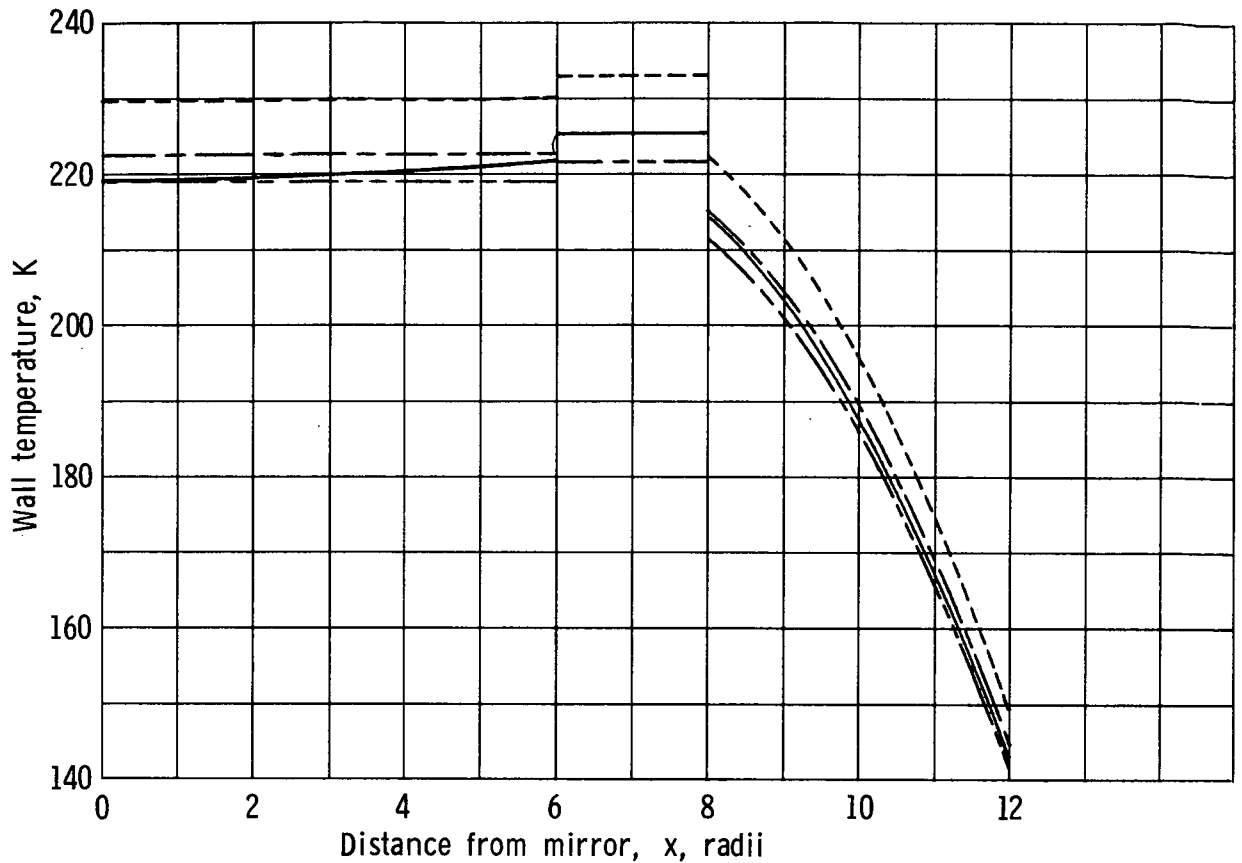
Line	Main-section temperatures, K		Collar temperature, T_c, K	$q = \sigma T_c^4$	Power input to collar	
	$x = 0$	$x = 6$			W/cm^2	$\dfrac{W}{(r = 150\ cm)}$
- - - -	229.75	230.20	233.07	$4 \quad \times 10^{-3}$	14.06×10^{-4}	398
——	222.60	222.75	225.42	3.5	12.12	343
*——	219.36	221.79	225.42	3.5	13.65	386
- — - —	219.04	219.04	221.69	3.268	11.21	317

*No external radiation input.

(a) $\alpha = 0.25$; $\epsilon = 0.85$.

Figure 8.- Temperature distribution along wall of open-ended tube with heated isothermal collar. k = 0.0025.
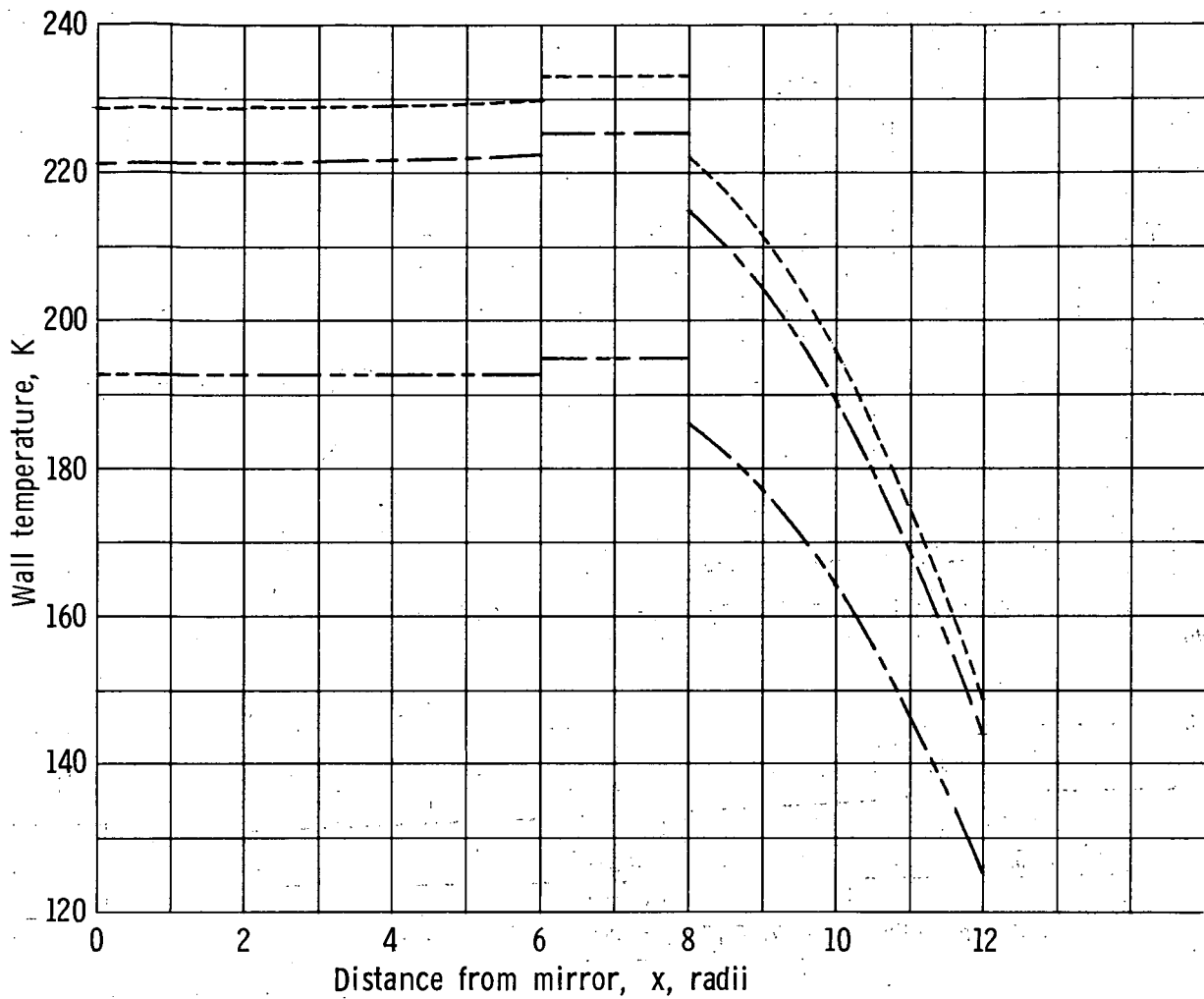
Line	Main-section temperatures, K		Collar temperature, T_c, K	$q = \sigma T_c{}^4$	Power input to collar	
	$x = 0$	$x = 6$			W/cm^2	W (r = 150 cm)
– – – –	228.59	229.85	233.07	4×10^{-3}	14.68×10^{-4}	415
————	221.32	222.37	225.42	3.5	12.73	360
– – —	192.78	192.78	195.02	1.961	6.73	190

(b) $\alpha = 0.15$; $\epsilon = 0.85$.

Figure 8.- Concluded.
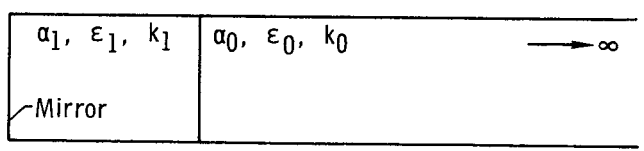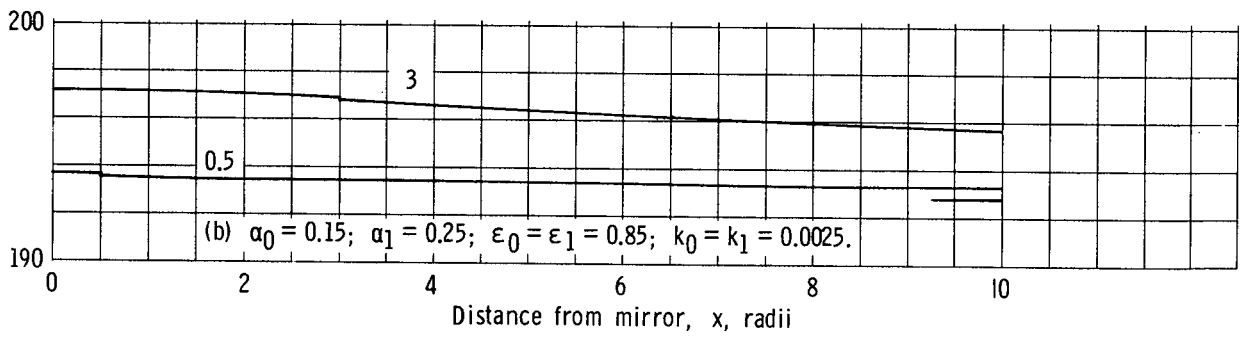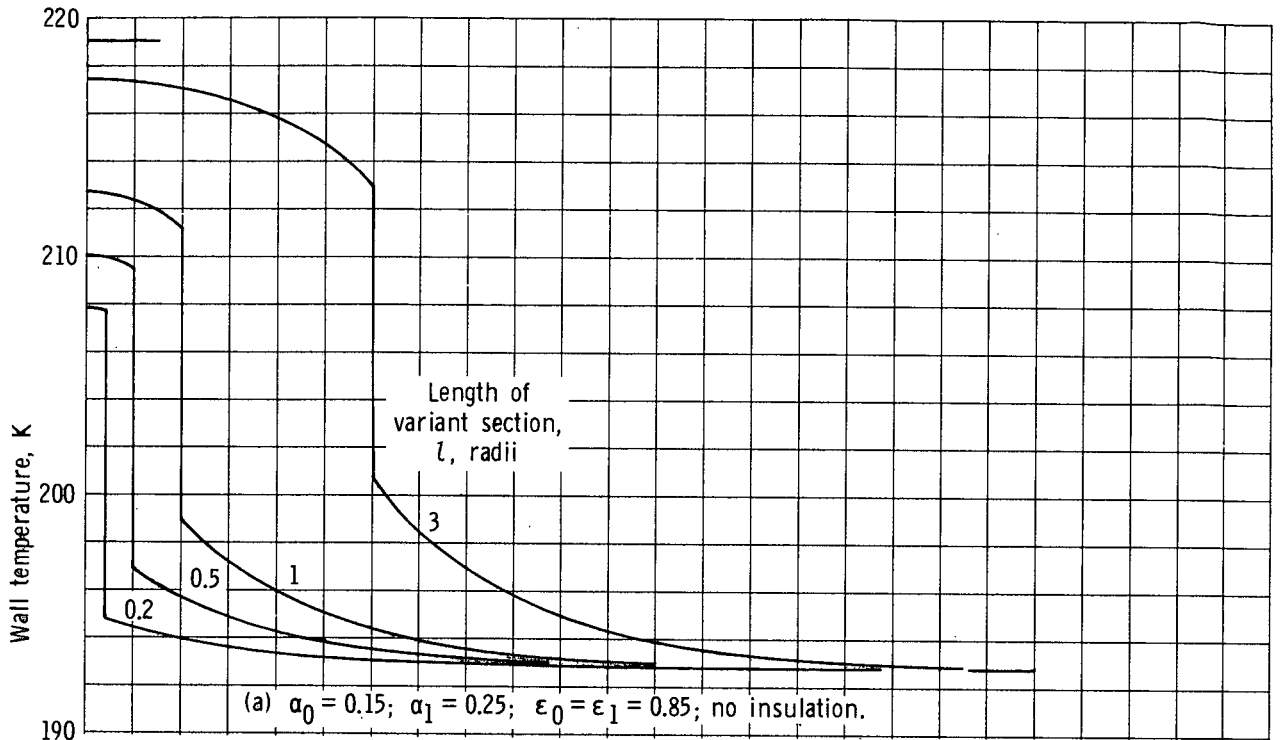
Figure 9.- Temperatures along wall of infinite cylinder having a short section with altered properties of the insulation, paint, or both. Cylinder axis normal to the solar rays. The short lines at the right indicate the asymptotic temperature — that is, the temperature in an infinite cylinder with the given values of α_0 and ϵ_0. The short lines at the left indicate the temperature in an infinite cylinder with the given values of α_1 and ϵ_1.

(c) $\alpha_0 = 0.15$; $\alpha_1 = 0.25$; $\varepsilon_0 = \varepsilon_1 = 0.85$; $k_0 = 0.025$; $k_1 = 0.05$.

(d) $\alpha_0 = 0.15$; $\alpha_1 = 0.25$; $\varepsilon_0 = \varepsilon_1 = 0.85$; $k_0 = 0.0025$; $k_1 = 0.005$.
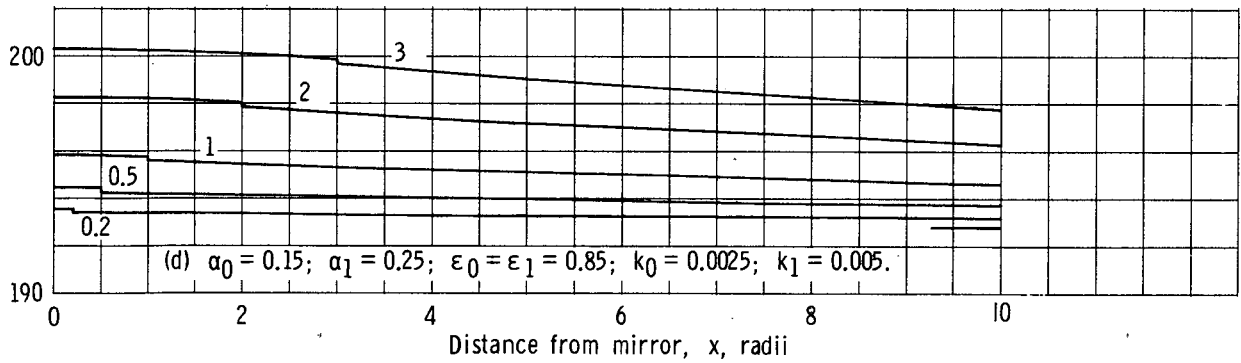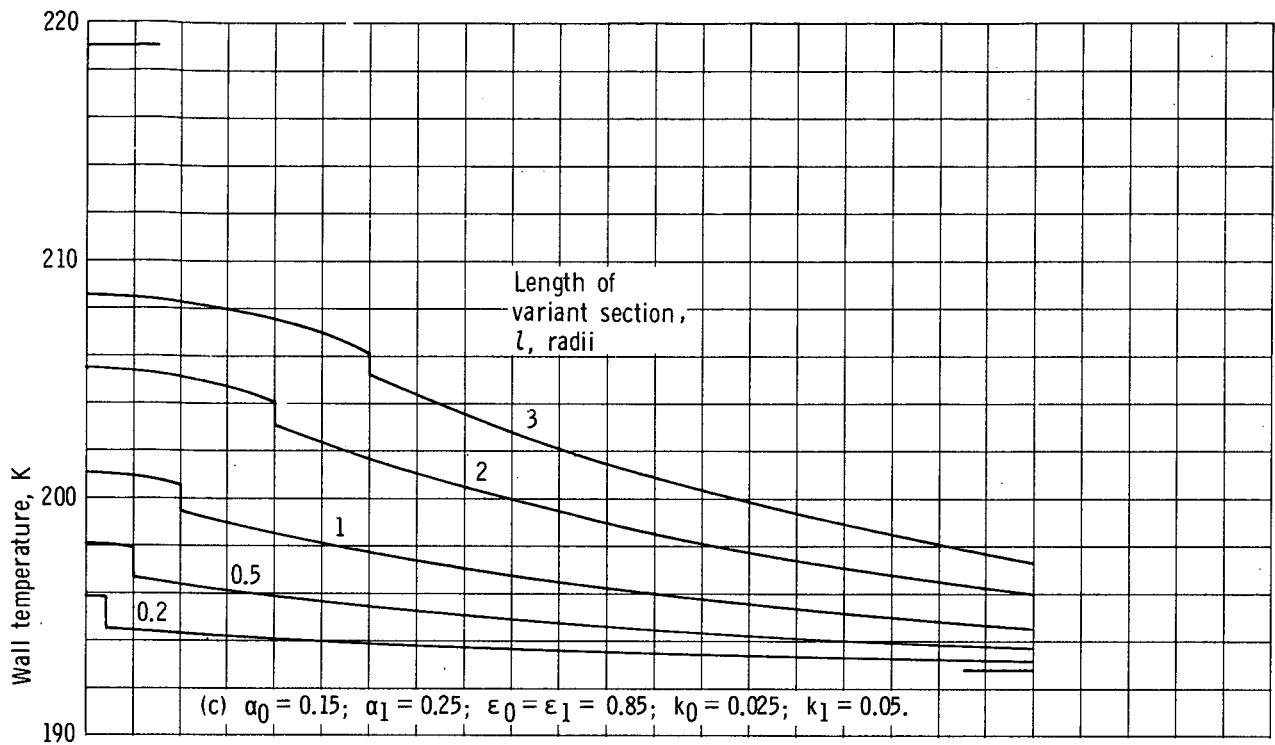
Figure 9.- Concluded.
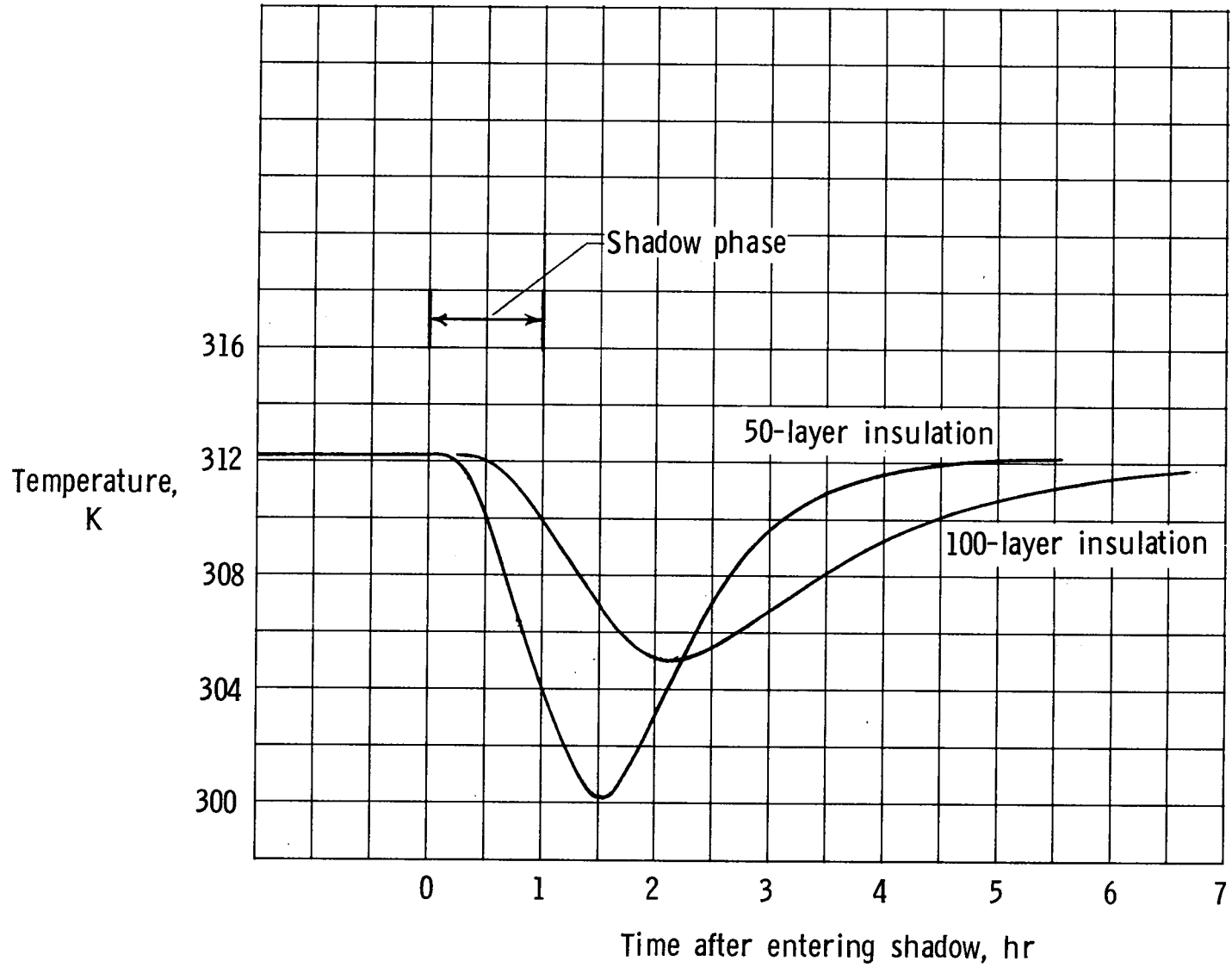
Figure 10.- Response to a 1-hour shadow phase of temperature of sheet adjacent to tube wall. Subsolar area; tube axis normal to solar rays; $\alpha/\epsilon = 1$; k = 0.0025; wall temperature, 297.4 K.
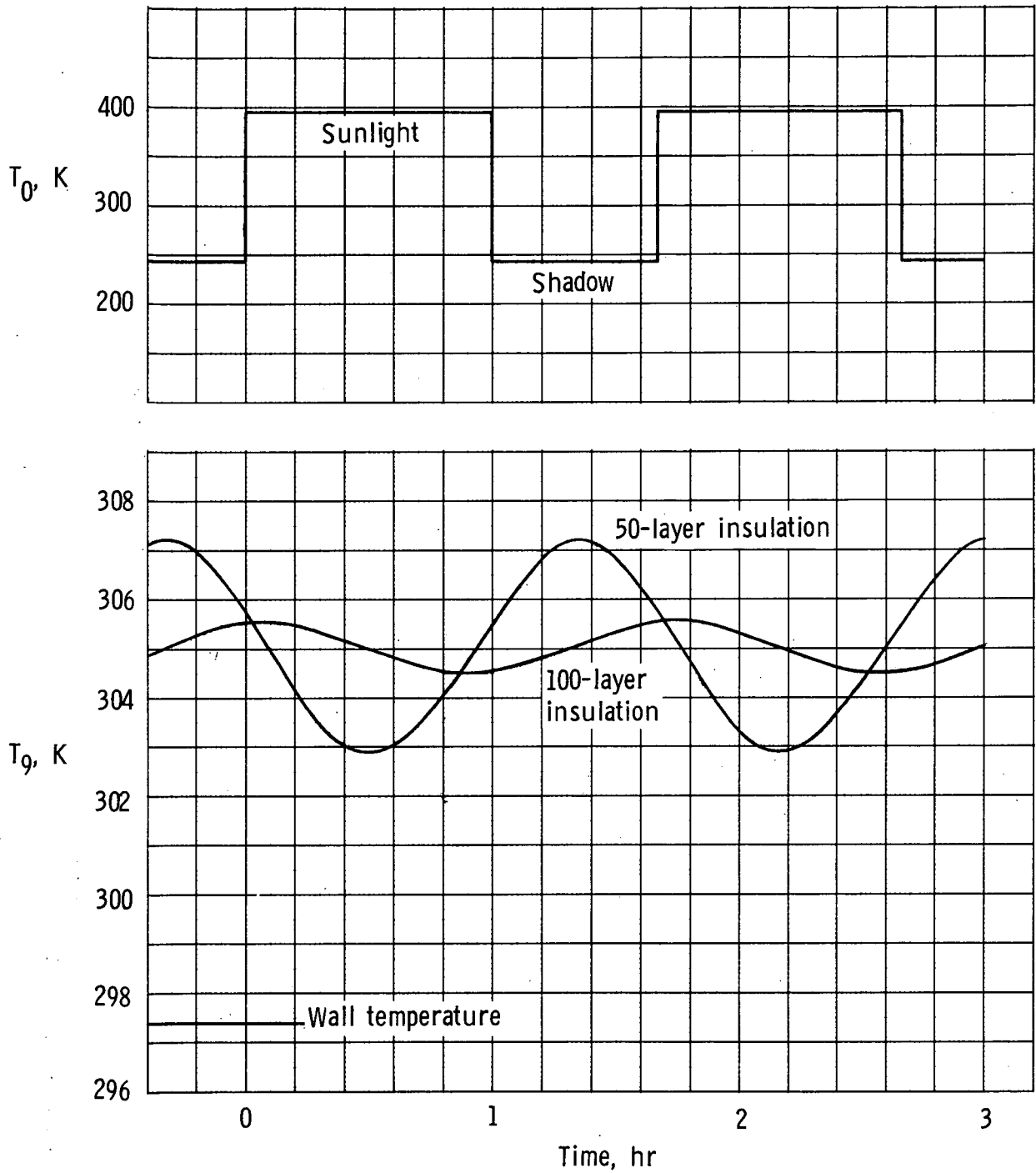
Figure 11.- Response to alternating 60-minute sunlight and 40-minute shadow phases of the temperatures of the outermost sheet $(T_0$, assumed) and of the sheet adjacent to the tube wall (T_9). Wall temperature, 297.4 K; k = 0.0025.